



Simulation of flows of viscoelastic fluids at high Weissenberg number using a filter-based stabilization of the spectral element method

Azadeh Jafari ^{*}, Nicolas Fiétier, Michel O. Deville

Laboratory of Computational Engineering, Institute of Mechanical Engineering, Ecole Polytechnique Fédérale de Lausanne, CH-1015 Lausanne, Switzerland

ARTICLE INFO

Article history:

Received 17 August 2010

Received in revised form 12 July 2011

Accepted 28 August 2011

Available online 28 September 2011

Keywords:

Viscoelastic fluid flows

High Weissenberg number

Spectral elements

Filter-based stabilization technique

ABSTRACT

The challenge for computational rheologists is to develop efficient and stable numerical schemes in order to obtain accurate numerical solutions for the governing equations at values of practical interest of the Weissenberg number. One of the associated problems for numerical simulation of viscoelastic fluids is that the accuracy of the results when approaching critical values at which numerical instabilities occur is very low and refining the mesh proved to be not very helpful. In order to investigate the numerical instability generation a comprehensive study about the growth of spurious modes with time evolution, mesh refinement, boundary conditions and Weissenberg number or any other affected parameters is performed on the planar Poiseuille channel flow. To get rid of these spurious modes the filter based stabilization of spectral element methods proposed by Boyd (1998) [1] is applied. This filter technique is very useful to eliminate spurious modes for one element decomposition, while in the case of multi-element configuration, the performance of this technique is not ideal. Since the performance of filter-based stabilization of spectral element acts very well for one element decomposition, a possible remedy to solve the associated problem of multi-element decomposition is mesh-transfer technique which means: first mapping the multi-element configuration to one element configuration, applying filter-based stabilization technique to this new topology and hereafter transferring the filtered variables to the original configuration. This way of implementing filtering is very useful for the Oldroyd-B fluids when a moderate number of grid points is used.

© 2011 Elsevier Ltd. All rights reserved.

1. Introduction

One of the worst obstacles for numerical simulation of viscoelastic fluids is the presence of spurious modes during the simulation. At high Weissenberg number, many schemes suffer from instabilities and numerical convergence may not be attainable. This is often attributed to the presence of solution singularities due to the geometry, the dominant non-linear terms in the constitutive equations, or the change of type of the underlying mixed-form differential system [2,3]. In the past two decades, considerable efforts have been devoted to the development of robust and stable numerical methods for simulating non-trivial flows of complex fluids. Without any exception, the standard viscoelastic models like Oldroyd-B, Maxwell, Phan-Thien-Tanner, FENE-P, etc. have failed in the simulation of high Weissenberg number flows in any available numerical techniques such as: finite difference, finite volume, finite elements, spectral elements, etc. [4].

In the framework of the spectral element method [5] for simulation of fluid flows, severe stability problems have also been encountered, especially when facing problems having low physical diffusion. Actually, spectral approximations are much less numerically diffusive than low-order ones and according to this drawback, even minor errors can make the simulation unstable. To remove nascent instabilities induced by numerical techniques or infirmity of constitutive equation, applying stabilization methods or filtering is possibly helpful.

Upwind techniques are introduced to ensure stability and prevent unphysical upstream propagation of disturbances. An example is provided by Marchal and Crochet [6]. They applied the so-called streamline upwind (SU) method to the constitutive equation, which consists of adding an artificial, first order, stream-wise diffusion term to the classical weak form of the constitutive equation. In the context of finite element methods, it was shown by Rosenberg and Keuning [7] that global upwinding techniques may produce inaccurate results in regions of steep velocity gradients. The streamline integration scheme, which in essence is a method of characteristics applied to the purely hyperbolic constitutive model, leads to stable and accurate stress predictions even close to singularities. The key advantage in using

* Corresponding author.

E-mail addresses: jafariA@cardiff.ac.uk (A. Jafari), [\(N. Fiétier\)](mailto:nicolas.fietier@inf.ethz.ch), [\(M.O. Deville\)](mailto:michel.deville@epfl.ch).

streamline integration is that it does not produce cross-stream diffusion, which can distort in a non-negligible way, the stress field near boundary layer regions.

The SUPG formulation [8] induces numerical damping in the constitutive equation which has the well-known effect of stabilizing the solution. This formulation has been used successfully by Chauvière and Owens for the benchmark problems relative to the steady flows of a sphere falling in a tube and past a cylinder in a channel, using spectral elements [9,10]. In these papers, additional stabilization has been obtained by using an element by element (EE) solving technique. This technique benefits from the hyperbolic character of the constitutive equation. First, the elements, are ordered according to their location along the streamline, then the constitutive equation is solved on each element, which makes possible the use of a direct solver. The inflow boundary conditions are obtained from the upstream elements determined by following the streamlines or the problem inflow boundary conditions.

Another alternative classical upwind method for finite element is the discontinuous Galerkin or Lesaint-Raviart method, which has been applied to viscoelastic flows by e.g. Fortin and Fortin [11]. The viscoelastic stress is approximated discontinuously from one element to the next. The discontinuous Galerkin approach has been shown to present stability and convergence properties similar to those of the SU method [12].

Gerritsma and Phillips [13,14] have recommended the use of discontinuous approximation of the extra-stress between spectral elements for non-smooth problems i.e. problems with singularities or stress boundary layers. They have claimed that a continuous extra-stress approximation cannot reproduce jumps in the velocity gradient approximation without generation of spurious oscillations in the whole computational domain. They have also suggested that the extra-stress approximation be at least the same as that of the velocity approximation within one spectral element on a non-staggered grid, so that a well-posed problem is obtained. Although they brought proofs of their statements only for Stokes flows, it is likely that such a formulation can be also applied to the viscoelastic stress tensor.

Another stabilization method is called the elastic-viscous stress-splitting (EVSS) method [15–17] which is based on adding an elliptic contribution in the weak form of the momentum equation. There are two principal features associated with this method, stress-splitting and recovery of velocity gradients. For smooth viscoelastic flows, Khomami et al. [18] have demonstrated that for steady state problems, the EVSS formulation coupled with upwinding for the constitutive equation (and likewise hp schemes), provides a more stable discretisation than a standard formulation (either Galerkin or EVSS/Galerkin) without upwinding. Marginal stability improvements are noted for EVSS above conventional stress equation treatments. In the same context, Rajagopalan et al. [17] have shown, for a wide range of solvent viscosities, that the EVSS scheme is more accurate and stable than two alternative choices, namely the viscous and explicit elliptic momentum equation (EEME) schemes.

Another modification, the so-called DEVSS (D stands for discrete) of the initial EVSS method has been proposed by Guénette and Fortin [19]. The formulation is based on the introduction of the rate of deformation tensor as an additional unknown and of an additional equation involving this variable. Contrary to the popular EVSS method, no change of variable is performed into the constitutive equation. The main advantage of this method relies on the fact that it extends to more complicated rheological models where it is difficult or impossible to perform a change of variable into the constitutive equation. Moreover, this method is easier to implement since the constitutive equation remains unaltered. Fan et al. [20] have proposed an alternative to the EVSS-based formulations related to the concept of Galerkin/least square

perturbations proposed by Franca and Stenberg [21]. The Galerkin/least-square method consists of adding to the usual Galerkin method terms that are functions of the residual of the Euler–Lagrange equations evaluated element wise. The added perturbation terms are designed to enhance stability of the original Galerkin method; since the Euler–Lagrange equations are satisfied by the exact solutions, consistency is preserved in this method.

Direct minimization of the discontinuous least-squares spectral element formulation is described by Gerritsma [22]. The new ideas presented in this paper consist of the weak coupling of the fluxes in the least-squares formulations instead of imposing weak continuity of the dependent variables. Furthermore, direct minimization is employed instead of the conventional variational least-squares formulation. This full least-squares method turns out to be very robust way to model viscoelastic flow problem.

A new mathematical framework presented by Surana et al. [23] based on h , p , k and variationally consistent integral forms is utilized to develop a finite element computational process for 2D steady polymer flows utilizing upper convected Maxwell model. Its significance is that the mathematical framework and least square computational process based on h , p and k is free of inherent and numerical diffusion.

Other stabilization methods have been proposed in the spectral element context like the so-called bubble stabilization technique by Canuto et al. [24] or collocation techniques with modified grid by Funaro [25]. According to our knowledge, until recently their use has been restricted to Newtonian flows.

A new method for stabilizing viscoelastic flows is proposed by Ma et al. [26] which is suitable for high-order discretizations. It employs a mode-dependent diffusion operator that guarantees monotonicity while maintaining the formal accuracy of the discretization. Other features of the method are: a high-order time-splitting scheme, modal spectral element expansions on a single grid, and the use of a finitely extensible non-linear elastic-Peterlin (FENE-P) model.

Boyd [1] proposed a simple filter which satisfies the same boundary condition. The key idea is to rewrite variables in term of new functions, derived from the modal basis, which individually satisfy homogeneous boundary conditions and then apply the filter to modify the coefficient of these basis functions by arbitrary numbers without disturbing the boundary conditions. The filtered variable is then be transformed back into the original Chebyshev or Legendre basis.

Fischer and Mullen [27] have proposed the same filter as Boyd but in nodal basis for spectral element methods to remove instabilities induced by the non-linear convection term in the momentum equation. The filter is applied after each time step on an element by element basis to both velocity and stress fields.

Fischer et al. [28] have employed the filter-based stabilization technique for development and implementation of an efficient spectral element code for simulating transitional flows in complex three-dimensional domains. Critical to this effort is the use of geometrically non-conforming elements that allow localized refinement in regions of interest, coupled with a stabilized high-order time-split formulation of the semi-discrete Navier–Stokes equations. Till now this filtering has been applied only to Newtonian flows.

The aim of this article is to investigate the filter-based stabilization technique for the simulation of viscoelastic flows. To investigate the instability generation, a comprehensive study about the growth of spurious modes with time evolution, boundary condition, mesh refinement, finite extensibility parameter and Weissenberg number has been done. Then we focus more on the mathematical property of the constitutive equation and observe the influence of various parameters. The effects of the filter-based stabilization technique to get rid of nascent instabilities are also

presented and discussed. The C++ toolbox SPECULOOS [29] has been used and adapted to carry out this analysis and corresponding simulations.

This paper is organized as follows. After this introductory section, the conservation equations and rheological models restricted to the FENE type are introduced in Section 2. Numerical methods are presented in Section 3. The proposed filter-based stabilization is described in Section 4. The Poiseuille test problem is introduced in Section 5. Section 6 is dedicated to general considerations concerning the results and an introduction to the two following sections. Results of computations without filtering are presented in Section 7. Section 8 deals with the presentation of results obtained with filtering. The last section is dedicated to conclusions.

2. Governing equations

In this section, we summarize the equations that govern the flow of a dilute polymer solution. The time evolution of the viscoelastic stress is described by the FENE-P model [30,31]. Like Newtonian fluids, the flow of complex fluids is governed by the equations of conservation of mass and momentum. The momentum equation is modified with respect to the Newtonian case in order to account for the additional contribution due to the viscoelastic stress tensor. The dimensionless equations are given by the following equations:

$$\nabla \cdot \mathbf{u} = 0 \quad (1)$$

$$\frac{\partial \mathbf{u}}{\partial t} + Re(\mathbf{u} \cdot \nabla) \mathbf{u} = \nabla \cdot \boldsymbol{\sigma} \quad (2)$$

with:

$$\boldsymbol{\sigma} = \boldsymbol{\tau} - p\mathbf{I} + 2R_\mu \mathbf{D} \quad (3)$$

The symbols $\boldsymbol{\sigma}$, \mathbf{I} and \mathbf{D} are respectively the Cauchy stress, identity and rate of deformation tensors. $\boldsymbol{\tau}$ is the viscoelastic stress, \mathbf{u} is the velocity field and p is the pressure. The rate of deformation tensor is defined by:

$$\mathbf{D} = \frac{1}{2}(\mathbf{V}\mathbf{u} + (\mathbf{V}\mathbf{u})^T) \quad (4)$$

with the superscript T indicating the transpose. The parameters R_μ and Re are the ratio of Newtonian solvent viscosity, μ_N , to the total viscosity, $R_\mu = \mu_N/\mu_t$, and the Reynolds number ($Re = \rho U L/\mu_t$), where $\mu_t = \mu_N + \mu_p$. The symbol μ_p represents the polymeric viscosity, whereas U and L are the reference velocity and length, respectively. Here a particular model of the finite extensible non-linear elastic (FENE) family is considered. This model is based on a molecular, coarse-grained treatment of the polymer molecules as a collection of beads and springs with finite extension. The model suggests that dilute polymer solutions are a mixture of the solvent and the polymer, where the solvent convects the polymer molecules that are assumed to behave like dumbbells connected by elastic springs that can stretch. In the limiting case of the spring being able to be stretched infinitely, the model becomes the simpler macroscopic Oldroyd-B model, which is less physical. In particular, finite extensibility makes the viscometric response of the polymer more agreeable with experimental observation [32].

The polymer stress for FENE-P model is defined as:

$$\boldsymbol{\tau} = \frac{1 - R_\mu}{We} \frac{1}{1 - (tr(\mathbf{C})/b^2)} \left(\mathbf{C} - \frac{\left(1 - \frac{tr(\mathbf{C})}{b^2}\right)}{K} \mathbf{I} \right) \quad (5)$$

where \mathbf{C} is the conformation tensor, which satisfies the following differential equation:

$$We \left(1 - \frac{tr(\mathbf{C})}{b^2}\right) \left(\frac{D\mathbf{C}}{Dt} - \mathbf{C} \cdot (\nabla \mathbf{u})^T - \nabla \mathbf{u} \cdot \mathbf{C} \right) + \mathbf{C} = \frac{\left(1 - \frac{tr(\mathbf{C})}{b^2}\right)}{K} \mathbf{I} \quad (6)$$

and K is defined as:

$$K = 1 - \frac{3}{b^2} \quad (7)$$

The symbol tr denotes the trace. The parameter b is related to the extensibility of the dumbbells. When $b \rightarrow \infty$ the FENE-P model is equivalent to the Oldroyd-B model. Finite extensibility of the polymer implies that [33]:

$$tr(\mathbf{C}) < b^2 \quad (8)$$

The Weissenberg number is defined as $We = \lambda U/L$, where λ is the relaxation time. The ratio L/U corresponds to the inertial time of the flow.

2.1. The extended matrix logarithm formulation (EMLF)

Two distinct constraints for the FENE-P equation are imposed: (i) the square of the corresponding finite extensibility parameter of the polymer must be an upper limit for the trace of the conformation tensor and (ii) the eigenvalues of the conformation tensor should remain positive at all steps of the simulation. Negative eigenvalues cause the unbounded growth of instabilities in the flow. According to our previous work [34], we have introduced a new method based on the transformation of the classical constitutive equation by resorting to two changes of variables. In the first stage, we transform the classical constitutive equation based on the conformation tensor, \mathbf{C} , to a new one based on the tensor \mathbf{J} defined hereafter, which satisfies the condition of Eq. (8) at each time step

$$\mathbf{J} = \frac{K}{1 - \frac{tr(\mathbf{C})}{b^2}} \mathbf{C} \quad (9)$$

In the second stage, we transform the tensor \mathbf{J} to a so called matrix logarithm conformation tensor \mathbf{H} , based on the idea proposed by Fattal and Kupferman [35,36] in order to obtain positive eigenvalues for the \mathbf{J} and \mathbf{C} conformation tensors, namely

$$\mathbf{H} = \ln(\mathbf{J}) \quad (10)$$

Results and figures shown in this study are based on this extended matrix logarithm formulation.

3. Numerical methods

The set of mass-momentum and constitutive equation is discretized in space with a spectral element method whereas a second-order scheme based on finite differences has been selected for the time discretization as described in Refs. [34,37]. The pressure grid using Gauss-Legendre points is staggered with respect to the velocity and viscoelastic stress grid using Gauss-Lobatto-Legendre points. The variables are approximated with expressions involving Lagrangian interpolation polynomial based on the quadrature collocation points. In the spectral element context the inf-sup condition is satisfied if $n_p = n_v - 2$, where n_p and n_v represent the polynomials order of pressure and velocity, respectively. No such condition has been clearly defined for the viscoelastic or conformation tensor subspace. In most computations relative to viscoelastic flows with spectral elements method, the velocity and viscoelastic stress grids are taken to be the same. For temporal discretization, we have used in particular the implicit second-order backward differentiation formula (BDF2) for the Stokes operator and the explicit second order extrapolation scheme (EX2) for non-linear terms [38]. A fully decoupled approach solving separately the mass-momentum and constitutive equation has been considered. The constitutive equation is integrated at the new time step for the configuration tensor using velocity terms obtained at the previous time step. The viscoelastic stress tensor expressed

in terms of the configuration tensor is then inserted as a source term into the momentum conservation Eq. (2). The mass-momentum system of equations is then solved for the velocity and pressure at the new time step $n + 1$ using a classical technique for the Navier–Stokes problem. A preconditioned conjugate gradient solver algorithm is used for solving the mass-momentum equations. The fractional step method [39] is applied to decouple the velocity computation from the pressure one [34,38].

4. Filter-based stabilization technique

Despite the success of the spectral element methods (SEM) to deal with incompressible flows as testified by many examples reported in the literature, e.g. [28,40–43], severe stability problems have also been encountered, especially when low physical diffusion is present. These problems result from the fact that spectral approximations are much less numerically diffusive than low-order methods, even minor errors and under-resolution can make the calculation unstable [44]. Numerous filtering and stabilizing techniques have been proposed to overcome the stability problem [8,13,14,24,25]. In the frame of spectral element approximations, it is however essential to preserve the inter-element continuity, as discussed in [1]. The most recent and successful filtering techniques in the framework of spectral element method for Newtonian fluid, specifically for large eddy simulation are those proposed by Fischer and Mullen [27] using a nodal basis and Boyd [1] using a modal basis. The former approach is based on interpolations in physical space: Given the variable v (e.g. velocity or stress components) on a Gauss–Lobatto–Legendre (GLL) mesh with $(N + 1)^d$ nodes per element (where d is the space dimension and N is the degree of the polynomial approximation in each direction), in each element one uses the polynomial interpolate to compute v at the N^d nodes–GLL mesh, so that one obtains a new polynomial approximation, the degree of which in each direction is then $N - 1$. Using this polynomial one interpolates back on the initial grid. This filtering procedure of the highest frequencies is applied at each time step. An important advantage of the technique is that inter-element continuity and boundary conditions are preserved.

In this study, to get rid of instabilities of viscoelastic fluids which are induced by either numerical origin or mathematical modeling of constitutive equations or coupling of both sources, we apply the filter-based stabilization technique at the end of each time step of mass-momentum and constitutive equations. The filtering operation is performed by applying a given transfer function to a modal basis as explained in the following section.

4.1. Description of the filter

In this section we adopt the notation of Section (5.4) of [45]. The modal basis introduced in the p-version of finite elements [1] is presented in its one-dimensional version, the extension to two and three dimensions being straightforward by the use of tensor products. It is built up on the reference parent element $\widehat{\Omega} = [-1; 1]$ of the spectral element method as:

$$\begin{aligned}\phi_0 &= \frac{1 - \xi}{2} & \phi_1 &= \frac{1 + \xi}{2} \\ \phi_j &= L_j(\xi) - L_{j-2}(\xi) & 2 \leq j \leq N\end{aligned}\quad (11)$$

where L_j is the Legendre polynomial of degree j . Unlike the Lagrange–Legendre nodal basis used in our spectral element calculations, this modal basis forms a hierarchical set of polynomials allowing to define in an explicit and straightforward manner a low-pass filtering procedure. Any variable v can be expressed in this basis by the relation:

$$v(\xi) = \sum_{j=0}^N \check{v}_j \phi_j(\xi) \quad \xi \in \widehat{\Omega} = [-1, 1] \quad (12)$$

where \check{v} is unknown variable in the modal basis. In matrix notation one reads:

$$\mathbf{v} = \Phi \check{\mathbf{v}} \quad (13)$$

where

$$\Phi_{ij} = \phi_j(\xi_i) \quad (14)$$

The filtering operation is performed in the spectral modal space through a diagonal matrix \mathbf{K} whose components are chosen in order to fulfill the required properties of the filter. The filtering process is expressed by:

$$\bar{\mathbf{v}} = \Phi \mathbf{K} \Phi^{-1} \mathbf{v} = \mathbf{G} \mathbf{v} \quad (15)$$

4.2. Transfer function

C^0 -continuity, conservation of constants, invertibility and low-pass filtering are obtained by properly choosing the transfer function represented by the diagonal transfer matrix \mathbf{K} . As the filter acts in a different basis from the one used for our spectral element calculations, C^0 -continuity is preserved if the boundaries of the elements are not affected by the filtering procedure. One can notice that the only shape functions having non-zero values at the element boundaries are ϕ_0 and ϕ_1 , while $\phi_j, j \geq 2$ are bubble functions. The functions ϕ_0 and ϕ_1 that are linear Lagrange interpolants are responsible for imposing the non-zero values on element edges. Therefore, the transfer function coefficients must satisfy the relationship:

$$K_{ij} = \delta_{ij} \quad i, j \leq 1 \quad (16)$$

with δ_{ij} the Kronecker operator. If K_{ij} verifies Eq. (16), the constants are conserved after filtering because they are expressed as a linear combination of ϕ_0 and ϕ_1 . The modal filter is not projective if all diagonal coefficients K_{ii} are non-zero. The last required property is to perform low-pass filtering in frequency. As this modal basis forms a hierarchical set of polynomials, low-pass filtering is done by damping the high-degree polynomial contributions. The transfer matrix is expressed by:

$$K_{ij} = \delta_{ij} K(i) \quad (17)$$

with the continuous transfer function

$$\kappa(k) = \frac{1}{1 + \left(\eta \frac{\max(0, k-n)}{N} \right)^2} \quad \eta \geq 0 \quad (18)$$

where η is a filtering rate and n is an integer constant depending on the constitutive equation. Here $\kappa(k) = 1$ for $k \leq n$. To satisfy the condition of Eq. (16), it is necessary to impose $n \geq 1$. To perform an appropriate low-pass filtering for viscoelastic fluids, first we computed the analytical spectrum of the constitutive equation in modal basis. We observed that for Poiseuille flows of Oldroyd-B and FENE-P fluids, one has to preserve the first three and four physical modes, respectively. According to this observation, $n = 2$ for Oldroyd-B and $n = 3$ for FENE-P model could be suitable values. To clarify, in Fig. 1, one element constant (unity) spectrum is filtered with three different shape functions at the filtering rate, $\eta = 10$. In this study we have used the two last ones (c) and (d) for Oldroyd-B and FENE-P models respectively. This shape of transfer function is similar to that one classically used in Refs. [45–47].

The effect of filtering rate, η , on 1-D unity spectrum for Oldroyd-B and FENE-P has been shown in Fig. 2. As it is obvious in this figure, the largest value of η means the sharpest shape of filtering for eliminating the contribution of high order modes. This is the reason why we chose $\eta = 10$ for this study.

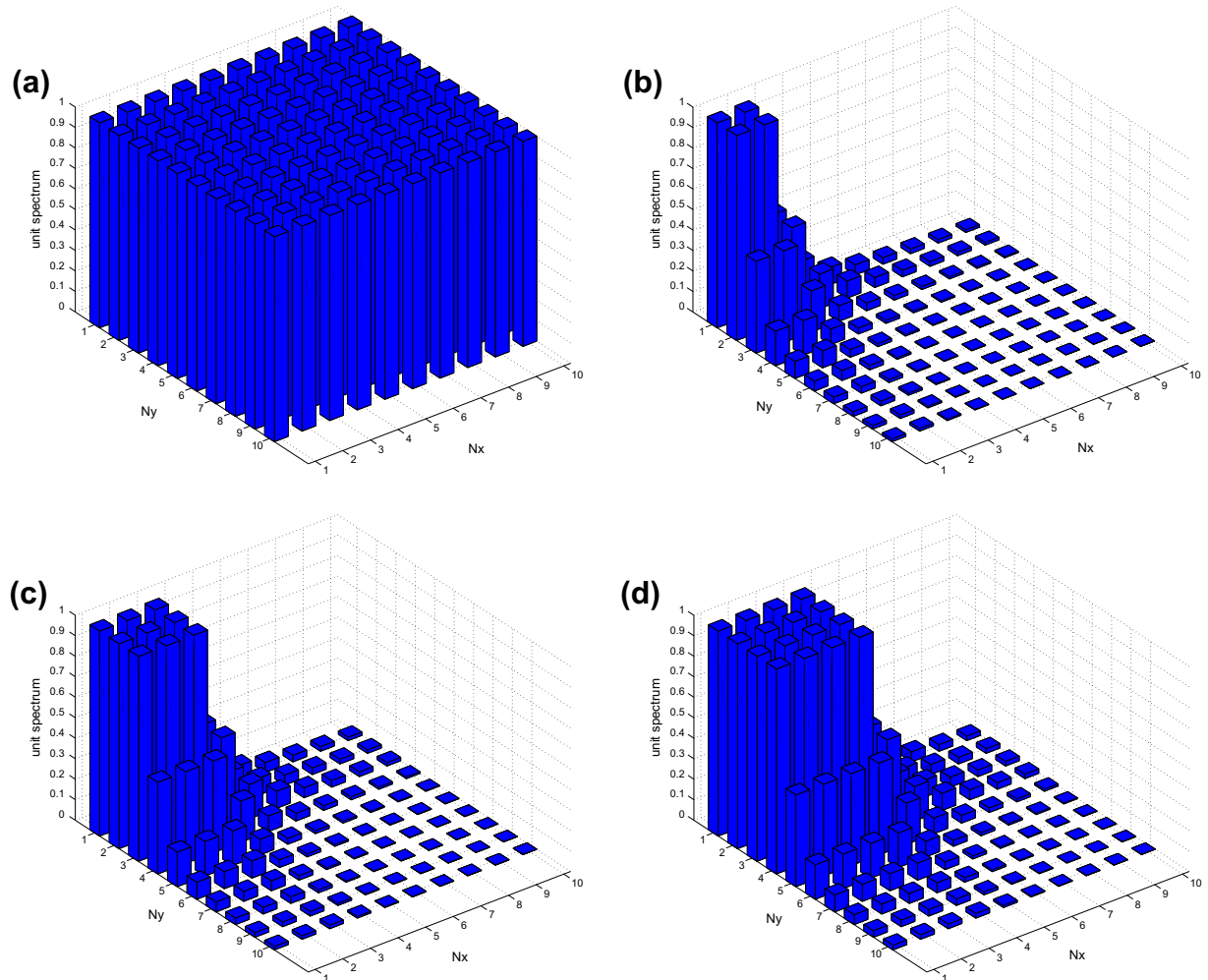


Fig. 1. Filtering one element unit spectrum, $\eta = 10$, (a) unit spectrum, (b) Newtonian fluids $n = 1$, (c) Oldroyd-B $n = 2$, (d) FENE-P $n = 3$.

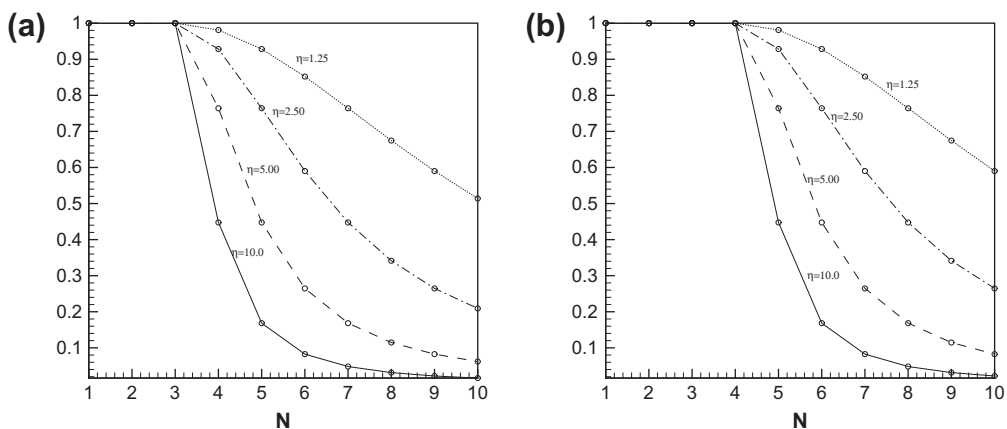


Fig. 2. Filtering 1-D unit spectrum for different values of the filtering rate, $\eta = 1.25$, $\eta = 2.5$, $\eta = 5$, $\eta = 10$, (a) Oldroyd-B, (b) FENE-P.

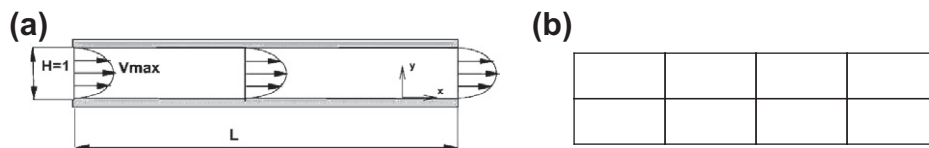


Fig. 3. (a) Poiseuille flow in a planar channel, (b) typical mesh decomposition.

5. Test problem

The steady planar Poiseuille flow (Fig. 3) is chosen as test problem. The simulation is performed by a transient algorithm that covers several thousands of time steps. It is expected that the steady solution remains stable in the long run.

Table 1

Maximum variation of modal spectrum of τ_{xx} with time evolution at $b^2 = 6$, $We = 100$, $(NE_x, NE_y) = (4, 2)$, $(N_x, N_y) = (6, 6)$ and natural outflow boundary condition.

Time step	1	5	7	11	13
$ \tau_{xx\text{analytical}}^* - \tau_{xx}^* $	10^{-3}	11	12	14	25

To observe the numerical instability generation, a study about the growth of spurious modes with time evolution, has been carried out. The effect of different parameters such as mesh refinement, boundary conditions, Weissenberg number, and finite extensibility has been investigated. To do so, first we compute the difference between the spectrum obtained by simulation and the one obtained analytically with time evolution for each variable in modal basis. The analytical spectrum of the modal basis has been derived from the full prescription of the steady flow. For the fluids of the FENE family in spite of the fact that no simple expression for the \mathbf{H} conformation tensor can be derived analytically, the constitutive equation becomes a set of non-linear algebraic equations, where for the fully developed Poiseuille flow the transverse component of the velocity is equal to zero and all quantities except the pressure are dependent on y only [34,38].

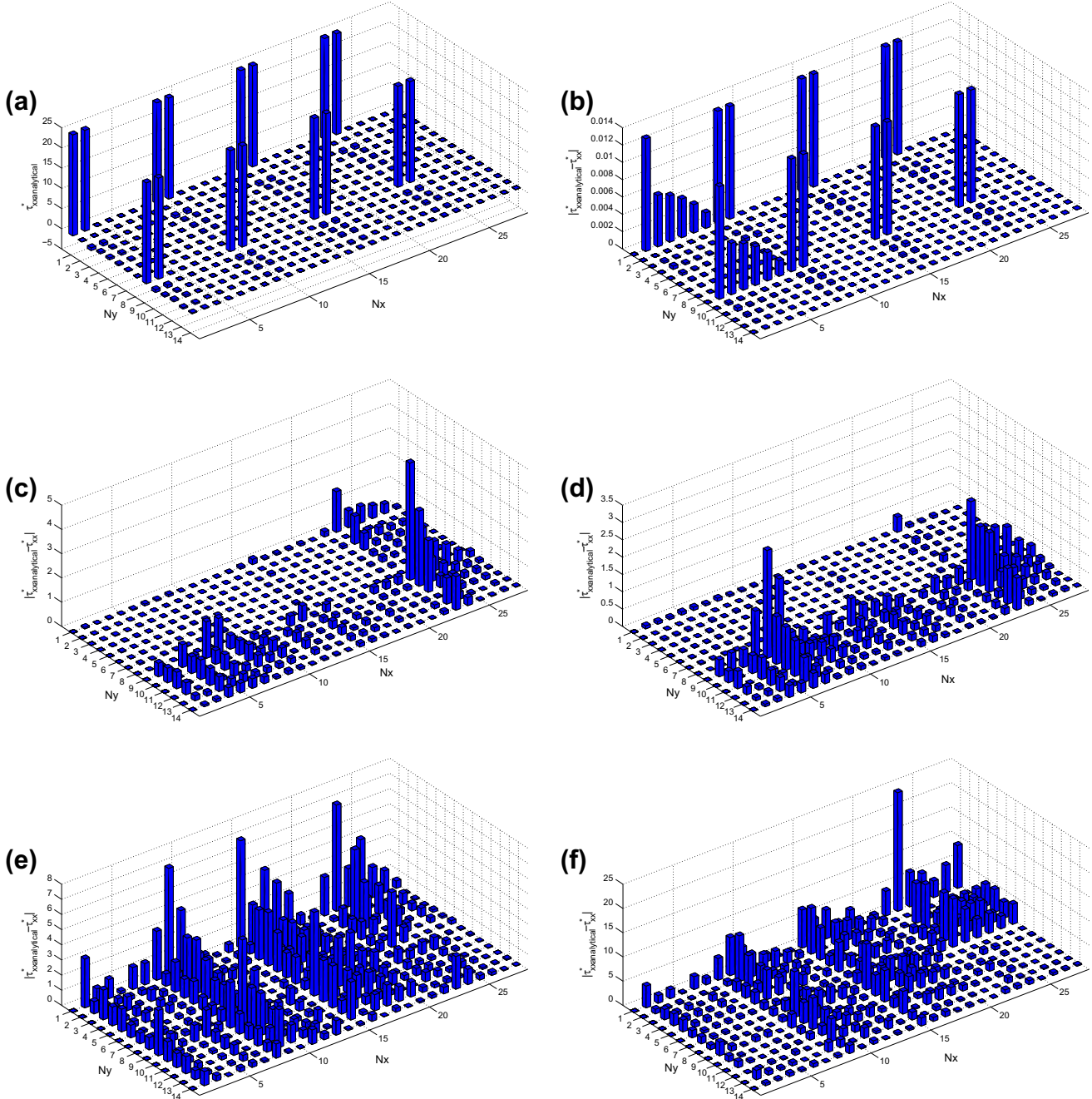


Fig. 4. Typical variation of modal spectrum of τ_{xx} with time evolution at $b^2 = 6$, $We = 10$, $(NE_x, NE_y) = (4, 2)$, $(N_x, N_y) = (6, 6)$ and natural outflow boundary condition: (a) full analytical prescription of the steady flow, (b) time step = 1, (c) time step = 101, (d) time step = 1001, (e) time step = 3001, (f) time step = 3180.

Analytical solutions are available for an Oldroyd-B fluid as reported in [38,48]. Moreover, to investigate the influence of element decomposition, we consider both multi-element and single element decompositions.

In the second stage, to get rid of these spurious modes, the filter-based stabilization of spectral element methods proposed by Boyd is applied to both FENE-P and Oldroyd-B fluids. Again, we consider both single and multi-element decompositions. This filter acts better for the single element comparing the multi-element decomposition. According to this fact, a new technique to apply this filter, the so called mesh-transfer technique, is proposed. The details of this method are explained in [45,49]. Let us summarize the main principles of mesh-transfer technique by following the notation of Bouffanais et al. To provide a new mesh topology, it is mandatory to transfer some information from the previous mesh to the new one. The main requirement imposed to this so-called mesh-transfer operation is to conserve the spectral accuracy of the SEM. As written in Section 3, the velocities and viscoelastic stress are expanded over a GLL grid and the pressure over a GL one. Therefore the mesh-transfer technique must be capable of transferring fields defined over GL and GLL grids.

Let us consider two meshes \mathcal{M}_1 and \mathcal{M}_2 corresponding to different mesh topology of the same computational domain and the mesh-transfer operation from \mathcal{M}_1 to \mathcal{M}_2 . In the sequel, the following decompositions in terms of spectral elements is assumed:

$$\Omega_i \cup \partial\Omega_i = \bigcup_{e=1}^{E_i} \Omega_i^e \quad \text{for } i = 1, 2. \quad (19)$$

As the computational domain remains unchanged, for each spectral element Ω_2^e , of \mathcal{M}_2 we have:

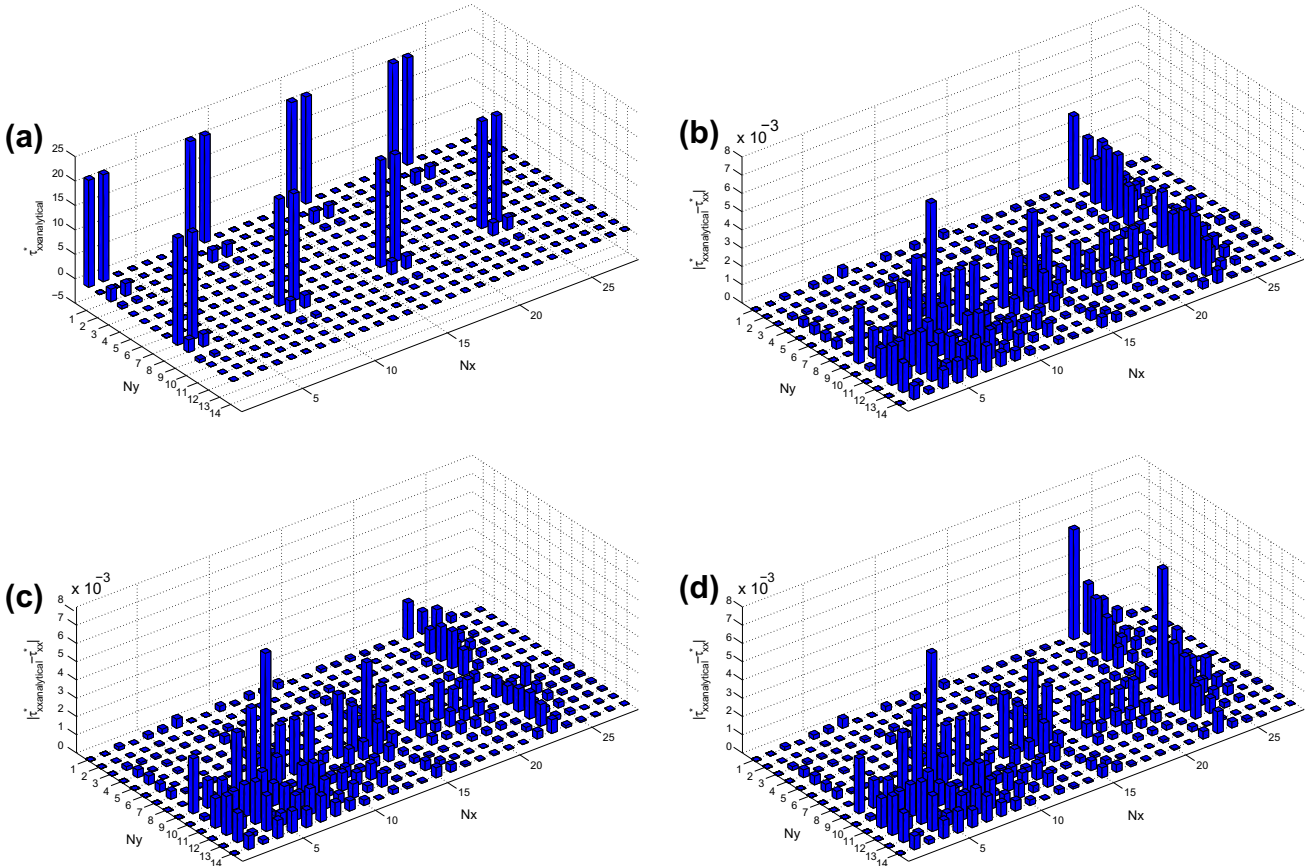


Fig. 5. Typical variation of modal spectrum of τ_{xx} with time evolution at $b^2 = 6$, $We = 1$, $(NE_x, NE_y) = (4, 2)$, $(Nx, Ny) = (6, 6)$ and natural outflow boundary condition: (a) full analytical prescription of the steady flow, (b) time step = 4501, (c) time step = 4801, (d) time step = 5000.

$$\Omega_2^e \subset (\Omega_1 \cup \partial\Omega_1) \quad \forall e = 1, \dots, E_2 \quad (20)$$

Due to Eq. (20) the mesh-transfer technique only requires an interpolation procedure. Let us note the physical location of the set of GLL grid points of a spectral element Ω_2^e , ($e_2 = 1, \dots, E_2$) by $\mathbf{x}_{ij,2}^{e_2}$ with ($i = 1, \dots, N_{x,2} + 1; j = 1, \dots, N_{y,2} + 1$, $N_{x,2}$ (resp. $N_{y,2}$) being the order of the polynomial interpolation in the x-direction (resp. y-direction) for the mesh \mathcal{M}_2 (with the same notations, $N_{x,2}$ and $N_{y,2}$ can be different from $N_{x,1}$ and $N_{y,1}$ respectively). The proposed algorithm can be summarized in three steps:

- Find the spectral element $\Omega_1^{e_1}$ of \mathcal{M}_1 containing $\mathbf{x}_{ij,2}^{e_2}$.
- Determine the position $\mathbf{r}_1^{e_1}$ of $\mathbf{x}_{ij,2}^{e_2}$ within the parent element $\hat{\Omega}_1^{e_1}$ of $\Omega_1^{e_1}$.
- Compute the value of the field at the point $\mathbf{x}_{ij,2}^{e_2}$ given $\mathbf{r}_1^{e_1}$, the GLL Lagrangian interpolation basis and the values of the field at the GLL grid points of $\Omega_1^{e_1}$.

\mathbf{x}_1 and \mathbf{r}_1 are the physical and parent coordinates respectively.

In the third stage, we focus on the mathematical property of the constitutive equation for the FENE-P family. We examine the effect of Weissenberg number, mesh refinement and time step. As we are using a time-dependent formulation in our simulations, they are started from a specified initial condition that is based on the prescription of the fully-developed steady flow for all variables by analytical (Oldroyd-B) or numerical (FENE-P). The computational domain consists of two parallel fixed walls. A constant non-zero pressure gradient is imposed on the flow. The magnitude of the applied pressure gradient is selected such that the channel flow rate is equal to one. All data plots shown correspond to $Re = 1$, $H = 1$, (channel height), $L = 4$, (channel length), $R_\mu = 1/9$, $b = \sqrt{6}$ unless

other values are explicitly stated. Dirichlet boundary conditions for velocity and viscoelastic stress, imposed at the inflow boundary, are obtained by computing a steady Poiseuille flow. At the outflow boundary, free conditions are applied. Free or natural boundary

condition means here that the velocity and viscoelastic stress tensor are not imposed on the outflow boundary. To compare the effect of outflow boundary on the results, a Dirichlet condition for the velocity field is also considered. No explicit boundary condition

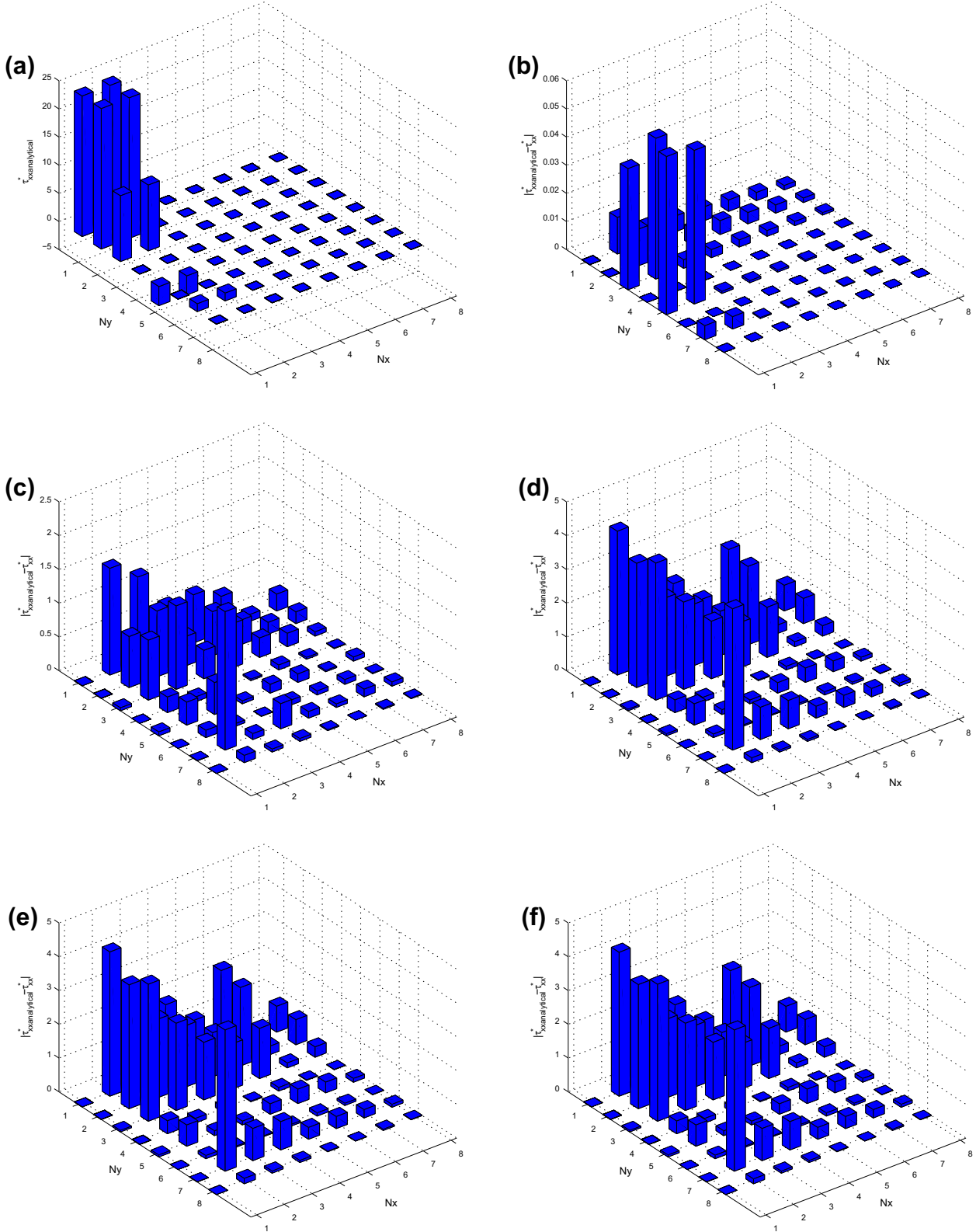


Fig. 6. Typical variation of modal spectrum of τ_{xx} with time evolution at $b^2 = 6$, $We = 10$, $(NE_x, NE_y) = (1, 1)$, $(N_x, N_y) = (7, 7)$ and natural outflow boundary condition: (a) full analytical prescription of the steady flow, (b) time step = 1, (c) time step = 101, (d) time step = 4001, (e) time step = 4501, (f) time step = 5000.

is imposed on the pressure since no pressure grid point lies on the boundary of the computational domain as a staggered grid is used for pressure.

Table 2

Maximum variation of modal spectrum of τ_{xx} with time evolution at $b^2 = 6$, $(NE_x, NE_y) = (1, 1)$, $(N_x, N_y) = (7, 7)$ and natural outflow boundary condition.

	Time step	1	101	1001	4001	5000
We = 100	$ \tau_{xx\text{analytical}}^* - \tau_{xx}^* $	0.03	1.50	1.00	3.00	2.50
We = 10	$ \tau_{xx\text{analytical}}^* - \tau_{xx}^* $	0.08	0.90	0.35	0.38	0.40

6. Results and discussion

The first part of the results is devoted to obtaining the modal spectrum of stream-wise velocity, first normal stress and shear stress at different times for the FENE-P model. These three variables are non-zero quantities in 2-D fully developed Poiseuille flow and the shape of their spectra is roughly the same while the corresponding magnitudes are obviously different. An investigation of the influence of various mesh and physical parameters has been carried out. However, for many cases because of instability problems, as the numerical simulation blows up before the total number of prescribed time steps (5000) is reached for a time step equal to $\Delta t = 0.002$, it was impossible to finish the computation

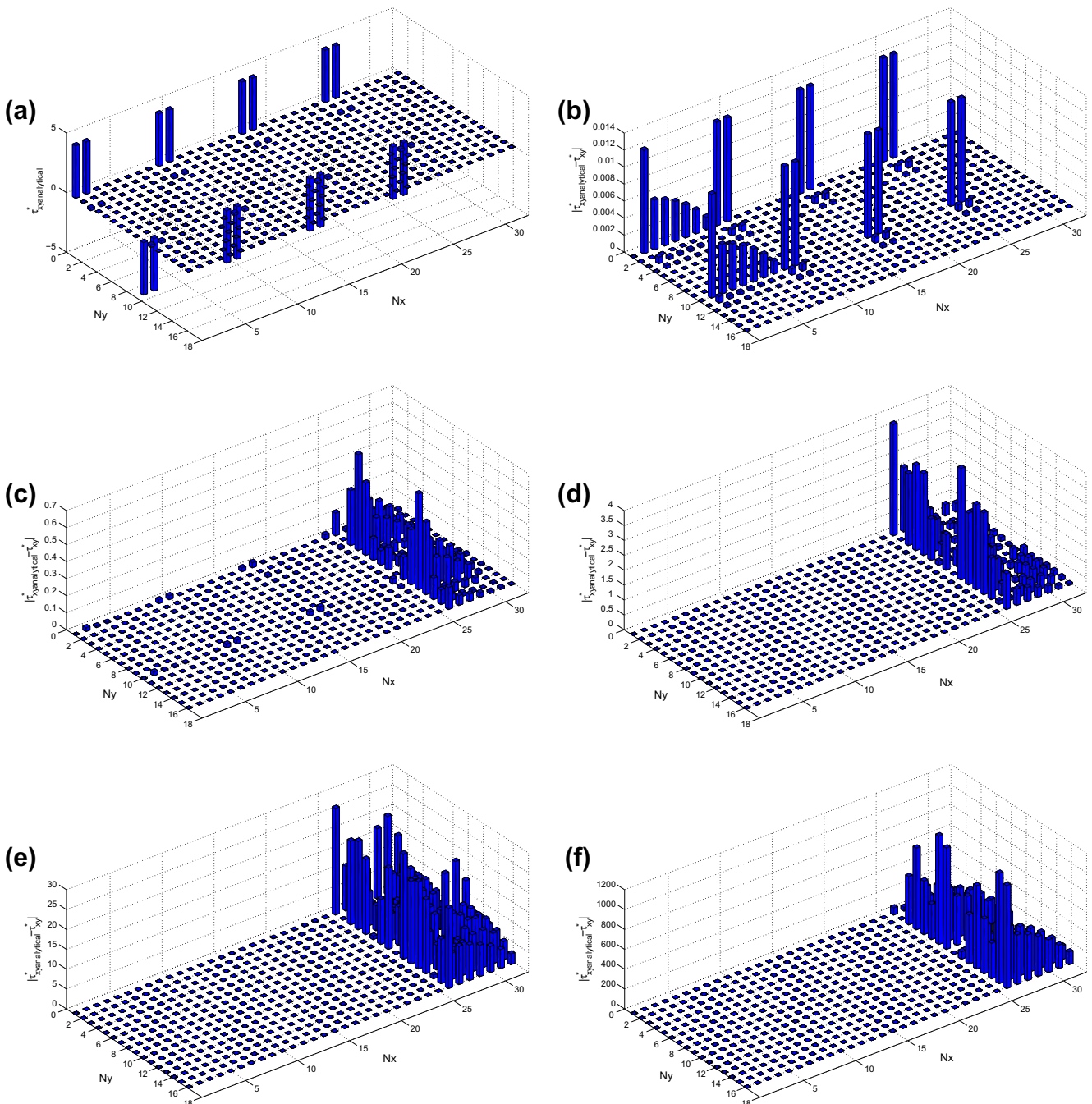


Fig. 7. Typical variation of modal spectrum of τ_{xy} with time evolution at $b^2 = 6$, $We = 1$, $(NE_x, NE_y) = (4, 2)$, $(N_x, N_y) = (7, 7)$ and natural outflow boundary condition: (a) full analytical prescription of the steady flow, (b) time step = 1, (c) time step = 10, (d) time step = 50, (e) time step = 100, (f) time step = 103.

Table 3

Maximum variation of modal spectrum of τ_{xy} with time evolution at $b^2 = 6$, $We = 1$, $(NE_x, NE_y) = (4, 2)$ and natural outflow boundary condition.

	Time step	1	2	15	25	34	35	45	56
$(N_x, N_y) = (8, 8)$	$ \tau_{xy}^{*}_{analytical} - \tau_{xy}^{*} $	0.01	0.25	–	3.50	–	–	4.50	3.50×10^9
$(N_x, N_y) = (10, 10)$	$ \tau_{xy}^{*}_{analytical} - \tau_{xy}^{*} $	0.01	0.70	3.00	–	200.00	5×10^5		

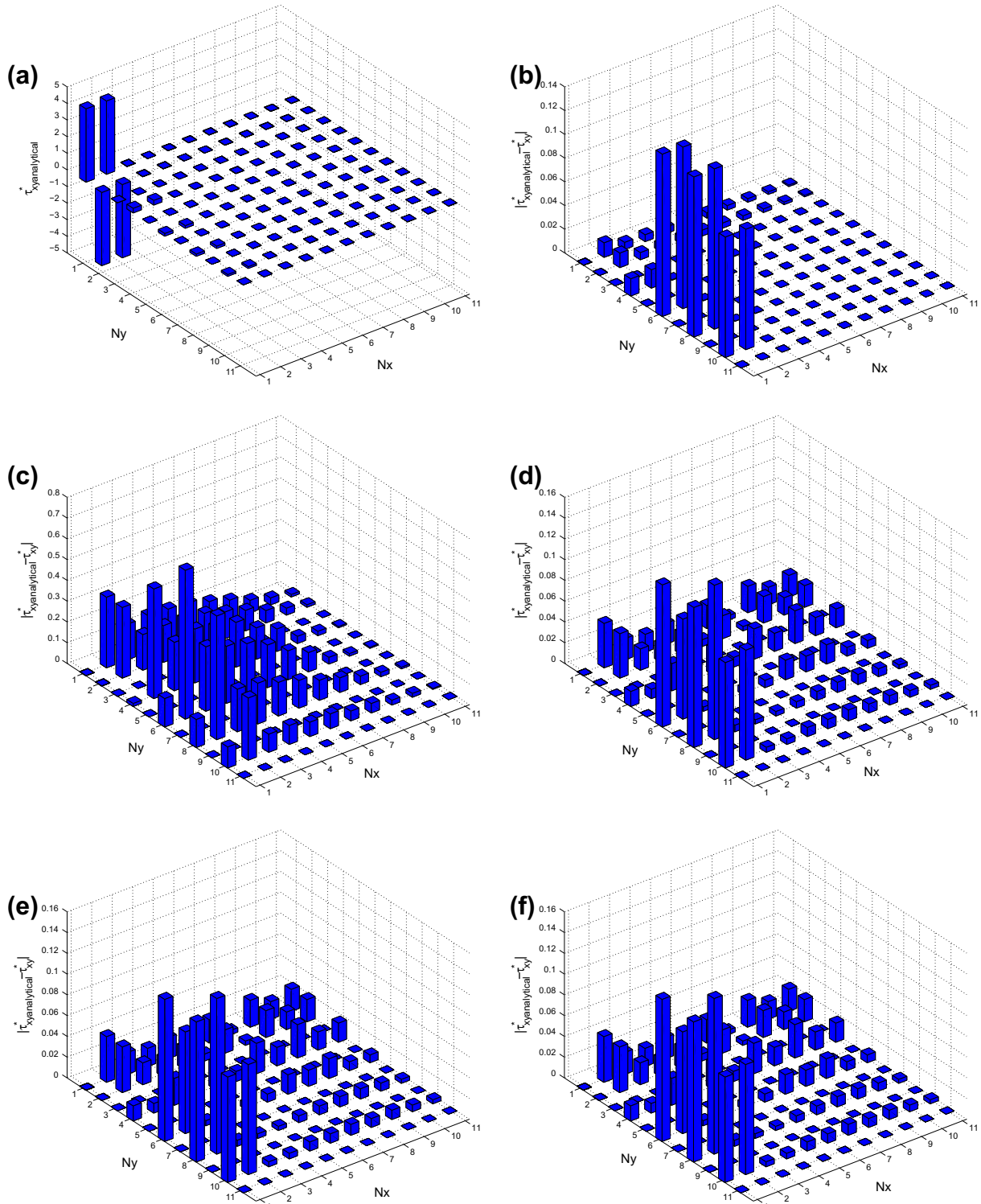


Fig. 8. Typical variation of modal spectrum of τ_{xy} with time evolution at $b^2 = 6$, $We = 1$, $(NE_x, NE_y) = (1, 1)$, $(N_x, N_y) = (10, 10)$ and natural outflow boundary condition: (a) full analytical prescription of the steady flow, (b) time step = 1, (c) time step = 101, (d) time step = 1001, (e) time step = 2001, (f) time step = 3000.

successfully. The first plot of each figure represents the spectrum of a component v^* of either the viscoelastic tensor or velocity, corresponding to the steady flow. The spectra of the difference $|v_{analytical}^* - v_{simulation}^*|$ is also represented at five different times where analytical corresponds here to the steady-state fully developed solution. First and last time steps are considered for every case, but for intermediate simulations, we pay more attention to the instant when unstable modes start to be significantly amplified. The variables in the captions of the figures and tables are

named with superscript '*' which means the spectrum of that variable expressed in the modal basis is considered.

Then in the second part of the study, we have applied a filter-based stabilization method to investigate the capability of this filter for the FENE-P and Oldroyd-B models. In contrast with the previous works, which employed the filter based stabilization method element by element, we propose a new way of implementation for global filtering as being explained in Section 5. The capability of this technique will be discussed with more details in the

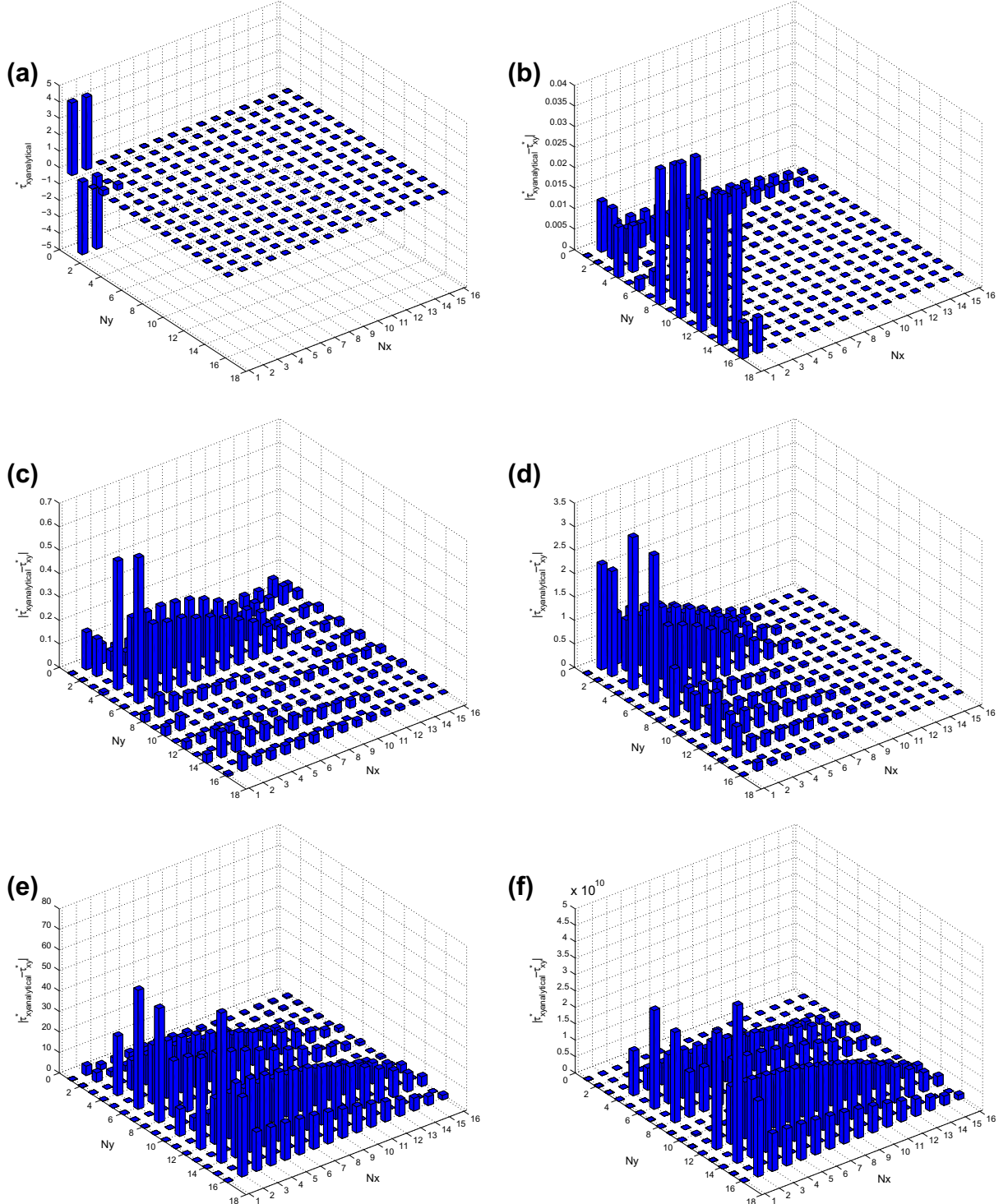


Fig. 9. Typical variation of modal spectrum of τ_{xy} with time evolution at $b^2 = 6$, $We = 1$, $(NE_x, NE_y) = (1, 1)$, $(Nx, Ny) = (15, 15)$ and natural outflow boundary condition: (a) full analytical prescription of the steady flow, (b) time step = 1, (c) time step = 5, (d) time step = 20, (e) time step = 50, (f) time step = 51.

following section. In the last part of this study we focus on the appearance of numerical instabilities for the FENE-P constitutive equation during the computation. Because of instability problems, the numerical simulation sometimes terminates before the final prescribed time.

7. Results without filtering

7.1. Influence of Weissenberg number

Table 1 corresponds to a Weissenberg number $We = 100$ and Figs. 4 and 5 represent the effect at $We = 10$ and $We = 1$ respectively. The corresponding time dependent simulations have been carried out for (4×2) elements and (6×6) polynomial degrees

in the stream-wise and cross-wise directions respectively with a natural outflow boundary condition. The reason for selecting (6×6) polynomial orders is that this is the maximum polynomial degree enabling completion of time dependent simulation at $We = 1$ with a natural boundary condition. These simulations are based on 5000 time steps with $\Delta t = 0.002$. However, for $We = 100$ and $We = 10$, because of instability problems, the numerical simulation stops at a smaller number of time steps. The first illustration in each figure represents the analytical spectrum of the full analytical prescription of the steady flow of first normal viscoelastic stress component. **Table 1** represents the maximum variation of the modal spectrum of the first normal stress with respect to the analytical one at time step 1, 5, 7, 11 and 13. The results show how fast the spurious modes are generated and amplified during the simulation for $We = 100$. We observed that the first excited

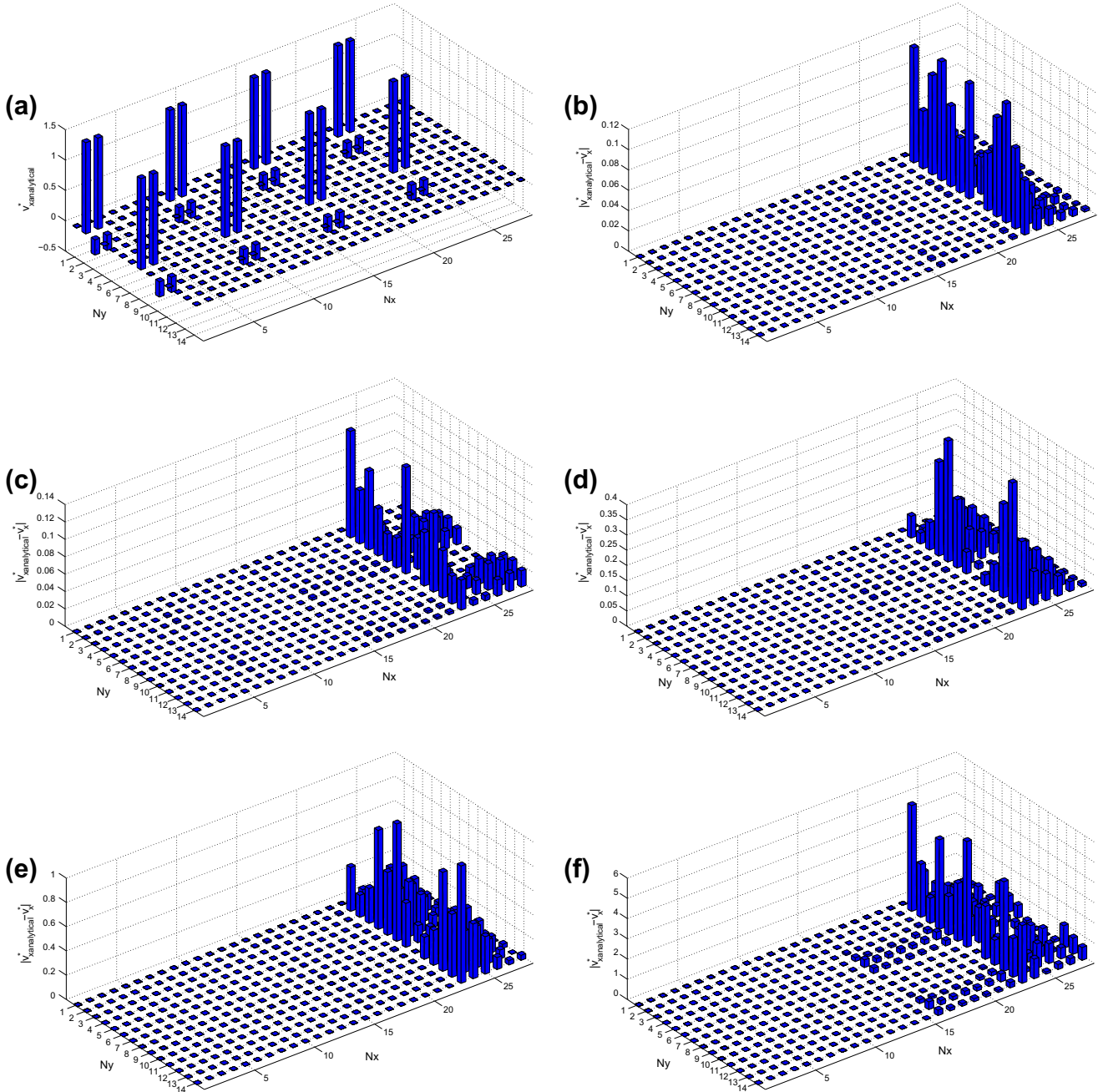


Fig. 10. Typical variation of modal spectrum of V_x with time evolution at $b^2 = 6 \times 10^6$, $We = 1$, $(NE_x, NE_y) = (4, 2)$, $(N_x, N_y) = (6, 6)$ and natural outflow boundary condition: (a) full analytical prescription of the steady flow, (b) time step = 1, (c) time step = 11, (d) time step = 21, (e) time step = 61, (f) time step = 121.

modes are induced at the last two elements near the outflow region and immediately penetrate upstream and cover the whole domain. At $We = 10$, Fig. 4, around time step 101, spurious modes induce a noticeable spectrum deviation from the analytical one and till time step 3180 where a significant difference between simulation and analytical values occurs, the numerical simulation can be performed. In the $We = 1$ case corresponding to Fig. 5, the simulation can be carried out successfully until step 5000 and the magnitude of unphysical modes at the end of the simulation is order of 10^{-3} .

The effect of Weissenberg number for single element at (7×7) polynomial degree are shown in Fig. 6 and Table 2. According to the fact that this is the maximum polynomial degree enabling completion of time dependent simulation for $We = 1$ with a natural outflow boundary condition, we chose this polynomial degree to investigate the influence of Weissenberg number on the modal spectrum. The magnitudes of spurious modes for $We = 100$, corre-

sponding to Table 2, and $We = 10$, corresponding to Fig. 6 for single element are lower than those obtained by the multi-element decomposition. The presence of these spurious modes causes a decrease of the accuracy of unknown variables at the end of the simulation.

7.2. Influence of mesh refining

Fig. 7 and Table 3 show the effect of mesh refining at $We = 1$ with outflow natural boundary condition for (4×2) element in stream and cross-wise direction respectively. Three different polynomial degrees (7×7) , (8×8) , and (10×10) are chosen for this test case with 5000 time steps and $\Delta t = 0.002$. For all the selected polynomial degrees, the simulation stopped before the prescribed number of time steps could be reached. As it is obvious in this figure the most excited modes are concentrated in two last elements close to the outflow region. These unphysical modes grow

Table 4

Maximum variation of modal spectrum of V_x with time evolution at $We = 1$, $(NE_x, NE_y) = (4, 2)$, $(N_x, N_y) = (6, 6)$ and natural outflow boundary condition.

	Time step	1	11	21	41	51	81	101	121
$b^2 = 60$	$ V_x^{*_{\text{analytical}}} - V_x^* $	0.10	0.12	0.35	–	0.70	80.00		
$b^2 = 6 \times 10^3$	$ V_x^{*_{\text{analytical}}} - V_x^* $	0.12	0.14	–	1.00	–	–	2.50	14.00

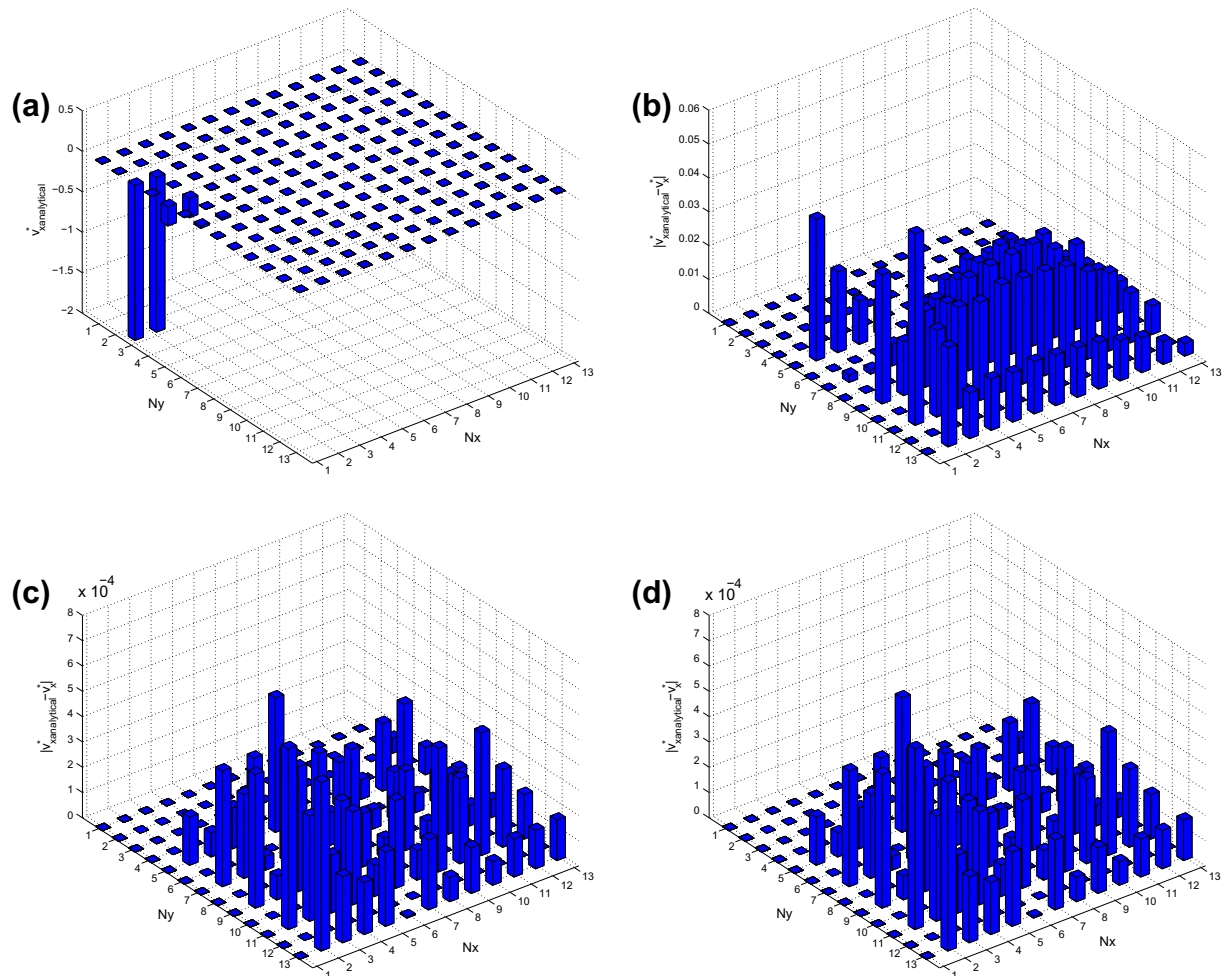


Fig. 11. Typical variation of modal spectrum of V_x with time evolution at $b^2 = 6$, $We = 1$, $(NE_x, NE_y) = (1, 1)$, $(N_x, N_y) = (12, 12)$ and natural outflow boundary condition: (a) full analytical prescription of the steady flow, (b) time step = 1, (c) time step = 4001; (d) time step = 5000.

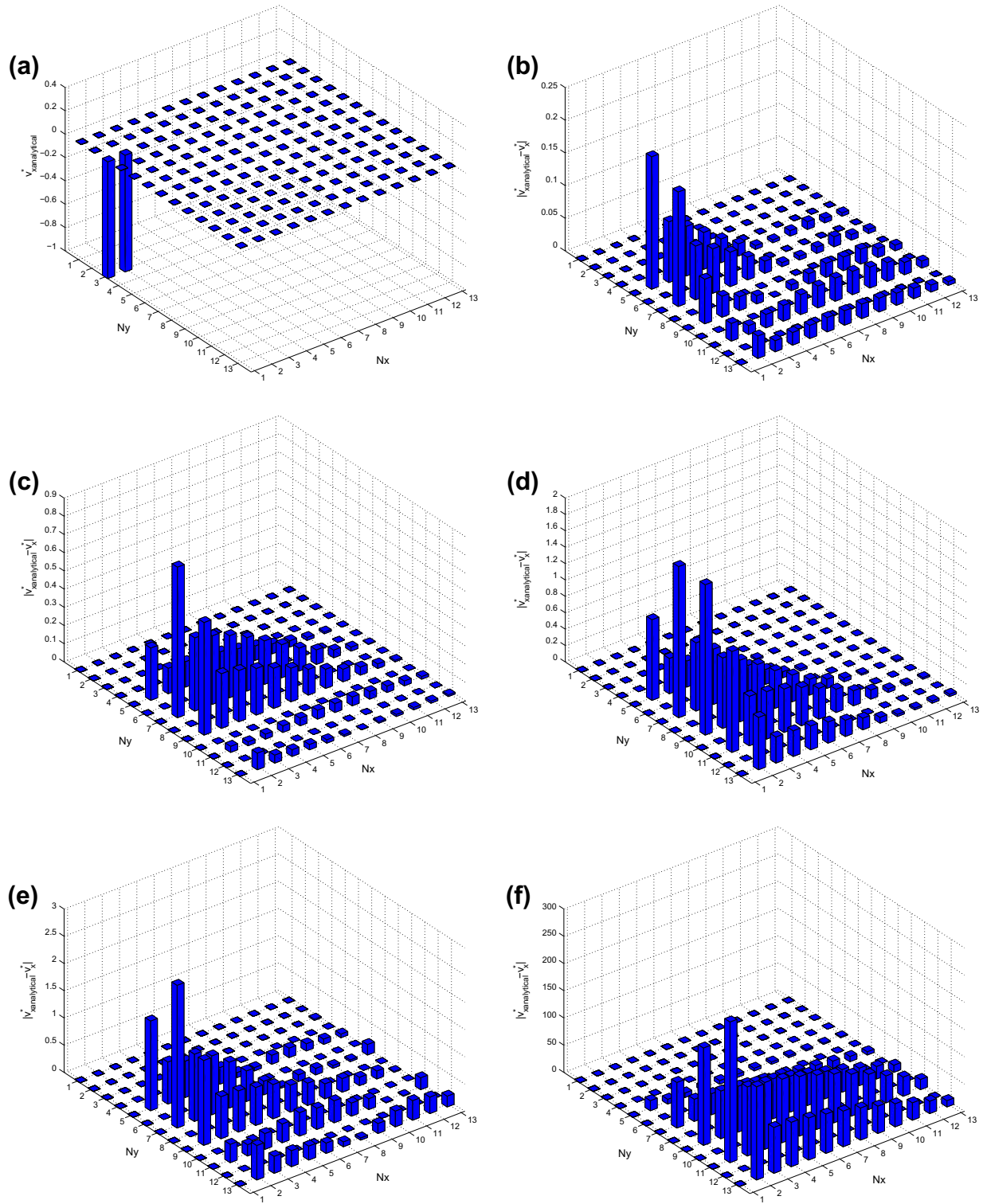


Fig. 12. Typical variation of modal spectrum of V_x with time evolution at $b^2 = 6 \times 10^6$, $We = 1$, $(NE_x, NE_y) = (1, 1)$, $(N_x, N_y) = (12, 12)$ and natural outflow boundary condition: (a) full analytical prescription of the steady flow, (b) time step = 1, (c) time step = 30, (d) time step = 100, (e) time step = 200, (f) time step = 219.

Table 5

Typical variation of modal spectrum of stream-wise velocity with time evolution at $We = 1$, $(NE_x, NE_y) = (1, 1)$, $(N_x, N_y) = (12, 12)$ and natural outflow boundary condition.

	Time step	1	25	30	50	100	114	200	280	310
$b^2 = 60$	$ V_x^*_{analytical} - V_x^* $	0.16	0.50	–	0.80	1.50	350.00			
$b^2 = 6 \times 10^3$	$ V_x^*_{analytical} - V_x^* $	0.23	–	0.85	–	–	–	3.00	3.30	2×10^{13}

very quickly and after 100 iterations the simulation blows up. As mentioned before for polynomial degree (6×6), one can carry out the simulation accurately as shown in Fig. 5. In fact, increasing the polynomial degree by only one order, from 6 to 7, significantly reduces the number of time steps that can be performed with the simulation. Discussion about this fact is postponed till Section 7.5.

The effect of mesh refining by increasing the polynomial degree is considered for the single element case at $We = 1$, and outflow natural boundary condition for (10×10) and (15×15) polynomial degrees. The maximum number of time step is chosen as 3000 with time interval equals to $\Delta t = 0.002$. On the corresponding Figs. 8 and 9, it may be observed again that the unphysical modes are triggered during the simulation. The magnitudes of these spurious modes are of the order of $O(10^{-1})$ and $O(10^{+10})$ respectively for

these two polynomial degrees. By increasing the polynomial degree the growth of spurious modes is enhanced and this is the reason why for (15×15) polynomial degree after 51 time steps the simulation breaks down, while for (10×10) polynomial degree the simulation can be carried out till 3000 time steps.

7.3. Influence of finite extensibility parameter

Let us now inspect the effect of the extensibility parameter, b , on the modal spectrum of the stream-wise velocity component. Fig. 10 and Table 4 represent the effect of finite extensibility parameter for (4×2) elements and (6×6) polynomial degree at $We = 1$ in the stream-wise and cross-wise directions respectively. The Oldroyd-B model can be considered as a particular case of

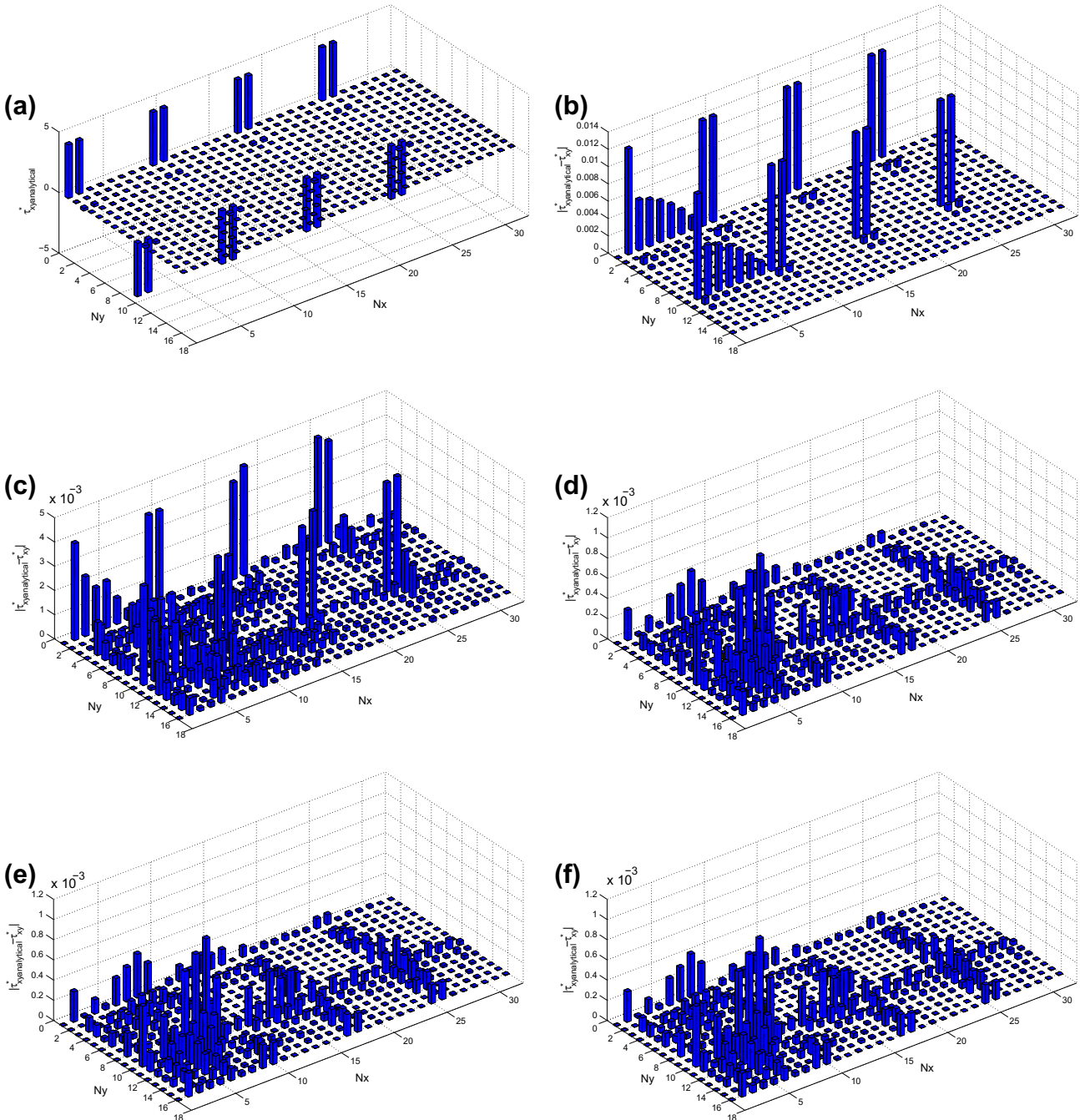


Fig. 13. Typical variation of modal spectrum of τ_{xy} with time evolution at $b^2 = 6$, $We = 1$, $(NE_x, NE_y) = (4, 2)$, $(N_x, N_y) = (7, 7)$ and Dirichlet velocity outflow boundary condition: (a) full analytical prescription of the steady flow, (b) time step = 1, (c) time step = 101, (d) time step = 1001, (e) time step = 2001, (f) time step = 3000.

the FENE-P model when $b \rightarrow \infty$. For all these three finite extensibility parameters $b^2 = 60$, $b^2 = 6 \times 10^3$, and $b^2 = 6 \times 10^6$, the numerical simulation blows up at some iteration number lower than the limit of 5000 whereas this limit could be reached for a value of the finite extensibility parameter equal to $b^2 = 6$ with the same conditions as shown in Fig. 5.

The influence of the finite extensibility parameter, b , on single element at $W = 1$ can be observed in Figs. 11 and 12 and Table 5. A natural outflow boundary condition and a spatial discretization with (12×12) polynomial degrees are selected. The reason for choosing this polynomial degree for this test case is that it is the maximum polynomial degree enabling completion of simulation

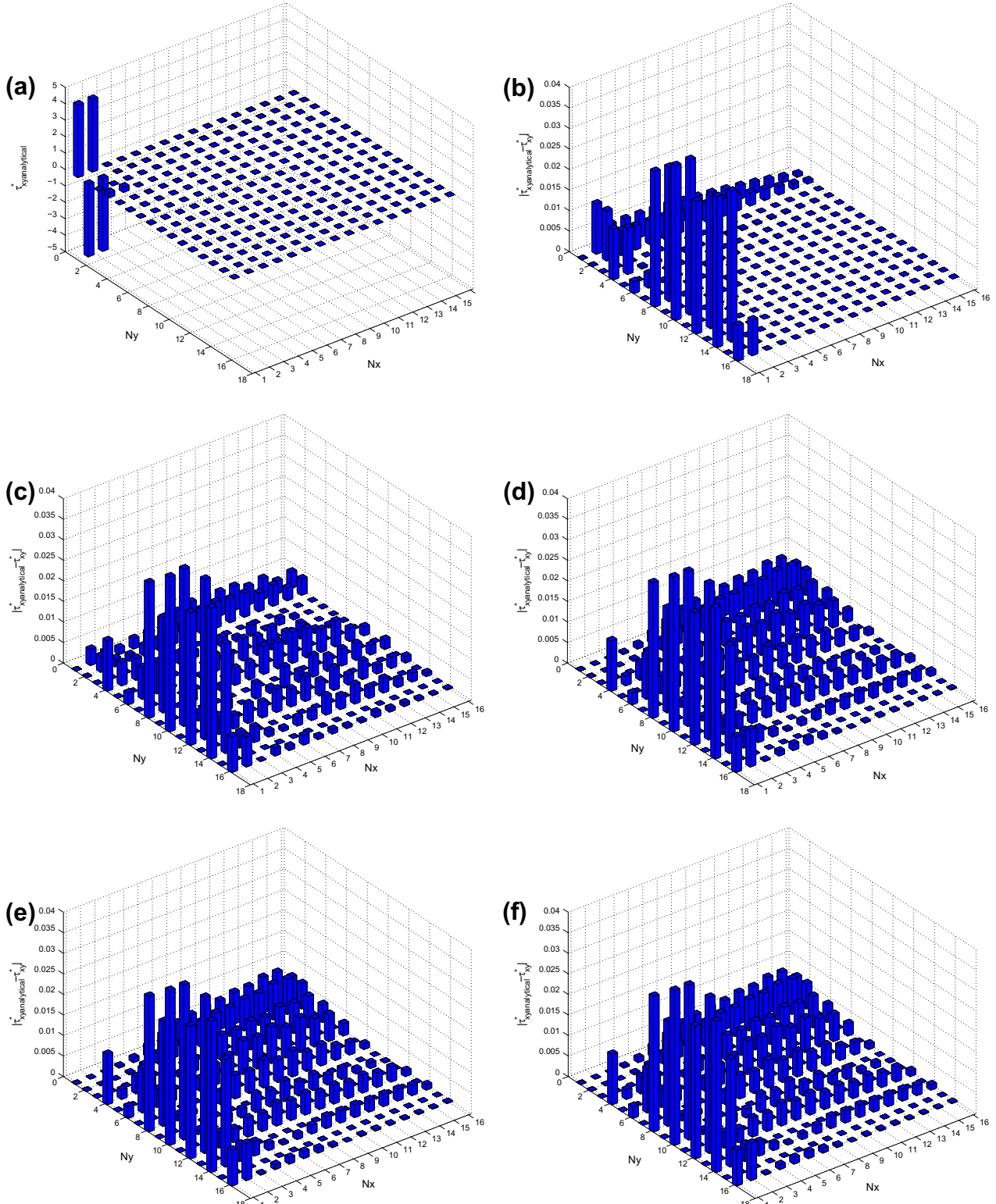


Fig. 14. Typical variation of modal spectrum of τ_{xy} with time evolution at $b^2 = 6$, $We = 1$, $(NE_x, NE_y) = (1, 1)$, $(N_x, N_y) = (15, 15)$ and Dirichlet velocity outflow boundary condition: (a) full analytical prescription of the steady flow, (b) time step = 1, (c) time step = 101, (d) time step = 1001, (e) time step = 2001, (f) time step = 3000.

at $We = 1$ and $b^2 = 6$ with this type of boundary condition. So by increasing the finite extensibility parameter we can investigate its effect on the modal spectrum. These test cases correspond to 5000 time steps as a maximum number of iterations with $\Delta t = 0.002$. For $b^2 = 6$, some spurious modes also grow during the simulation but the maximum difference in magnitude between the numerical spectrum and analytical one is of the order of $O(10^{-4})$ so one can obtain satisfactory results. Increasing the finite extensibility increases the magnitude of spurious modes and

causes the simulation to stop before the prescribed limit of number of time steps.

7.4. Influence of the outflow boundary condition

The influence of the outflow boundary condition at $We = 1$ can be observed in Figs. 13 and 14. Here, only a Dirichlet boundary condition for the velocity at outflow is considered (nothing imposed for the viscoelastic stress tensor). Fig. 13 corresponds to (4×2) elements and (7×7) polynomial degree in stream-wise and cross-wise direction. The main reason for selecting this polynomial degree is that it is impossible to perform simulations with this polynomial order for a natural boundary condition at $We = 1$, so we are interested in investigating the effect of a different outflow boundary condition on the results in terms of stability. In Fig. 14, we consider a single element and (15×15) polynomial degrees for $We = 1$, with the same Dirichlet boundary condition. This analysis has been done with 3000 time steps as a maximum number of iteration at $\Delta t = 0.002$. Comparison of Figs. 13 and 7 reveals that the numerical simulation is sensitive to the outflow boundary condition. Actually, by imposing a Dirichlet velocity boundary condition at outflow one can terminate the time dependent simulation successfully and accurately enough. The order of the error induced by the spurious modes at the end of simulation is of the order of $O(10^{-3})$ for the shear stress. The same conclusion holds for a single element discretization by comparing Figs. 14 and 9.

It is clear that the outflow boundary condition has very important effects on the manifestation of instabilities. Imposing a natural boundary condition introduces instability first in elements which

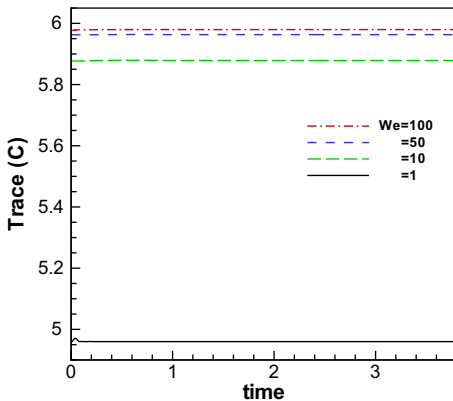


Fig. 15. Influence of the Weissenberg number on the maximum of $tr(C)$, $(NE_x, NE_y) = (4, 2)$, $(N_x, N_y) = (4, 5)$, natural outflow boundary condition: $\Delta t = 0.002$.

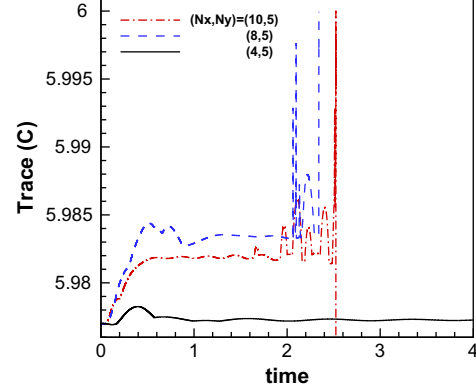


Fig. 16. Influence of mesh refinement on the maximum of $tr(C)$, $(NE_x, NE_y) = (4, 2)$, $We = 100$, natural outflow boundary condition: (left) $\Delta t = 0.002$, (right) $\Delta t = 0.0002$.

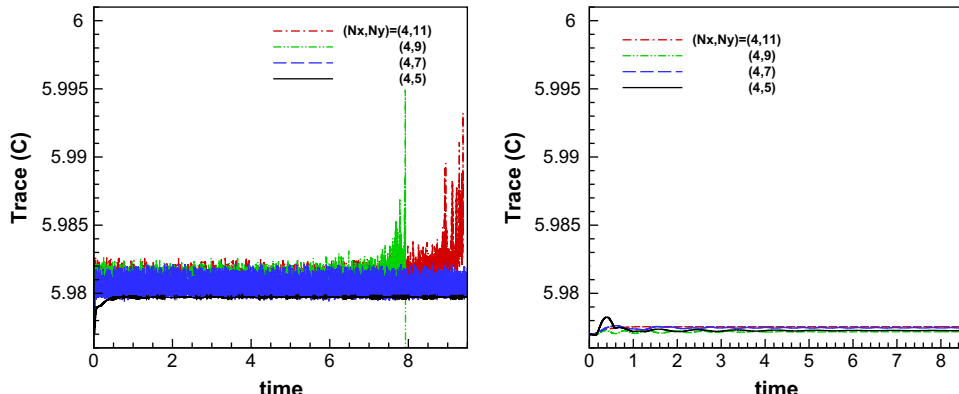


Fig. 17. Influence of mesh refinement on the maximum of $tr(C)$, $(NE_x, NE_y) = (4, 2)$, $We = 100$, natural outflow boundary condition: (left) $\Delta t = 0.002$, (right) $\Delta t = 0.0002$.

are close to the outflow region and afterwards these spurious modes penetrate upstream very fast. So imposing Dirichlet velocity boundary at outflow was found better in term of convergence and stabilization. The authors would like to emphasize that imposing periodic boundary condition for both velocity and viscoelastic stress at inflow and outflow, induces the same effect in reducing the growth of instabilities alike imposing only Dirichlet velocity boundary condition at outflow.

7.5. Influence of the time step

In a previous study [34], we provided a modification of the matrix logarithm formulation of Fattal and Kupferman [35,36], in order to preserve the positive eigenvalues of the conformation tensor at each time step and also to upper-bound the trace of the conformation tensor by the square of the finite extensibility parameter. However, this new formulation which conserves symmetric positive definiteness of the conformation tensor and also bounds the maximum value of the trace of the conformation tensor, can be helpful but there are still problems of instabilities. Regarding the mathematical model for the FENE-P family Eq. (6), in the denominator of the formulation, $1 - tr(C)/b^2$ appears. Whenever the computational value of $tr(C)$ is very close to b^2 , the denominator of the equation tends to zero. On the other hand, the viscoelastic stress tends to infinity, which does not have any physical meaning. In this study we do not try to improve the formulation and restrict ourselves to investigating the effect of Weissenberg number and mesh refinement on the computed value of the maximum of the trace of the conformation tensor. In the following we will show that one of

the reason for instabilities in FENE-P fluids is when the trace of the conformation tensor is very close to b^2 . We would emphasize that figures shown in this section are obtained with the natural boundary condition, while the same behavior is observed for the velocity Dirichlet condition at outflow. Results reported in this section are obtained with two different time steps, $\Delta t = 0.002$ and $\Delta t = 0.0002$. Because of explicit time marching scheme for the non-linear terms in momentum and constitutive equations, the Courant Friedrichs-Lowy (CFL) stability condition should be satisfied during the simulation

$$\max_k |\lambda_k \Delta t| = S \cdot CFL \quad (21)$$

where

$$CFL = \max_{c, \Delta x} \frac{c \Delta t}{\Delta x} \quad (22)$$

λ_k is the eigenvalue of the problem, c is the propagation speed, and S is an order-unity coefficient that depends on the discretization. For the spectral element method S is a non-linear function of N [5] (see Fig. 3.5.2 of this reference). We would emphasize that the CFL condition in this study is always met and the presence of instability reported in this section is observed for time steps satisfying the CFL number.

Fig. 15 represents the effect of the Weissenberg number on the maximum of the trace of the conformation for time intervals, $\Delta t = 0.002$. This test case has been done for (4×2) elements and (4×5) polynomial degrees in the stream-wise and cross-wise directions. As we suppose before, the attained maximum of $tr(C)$ increases by increasing the Weissenberg number. At $We = 100$, its

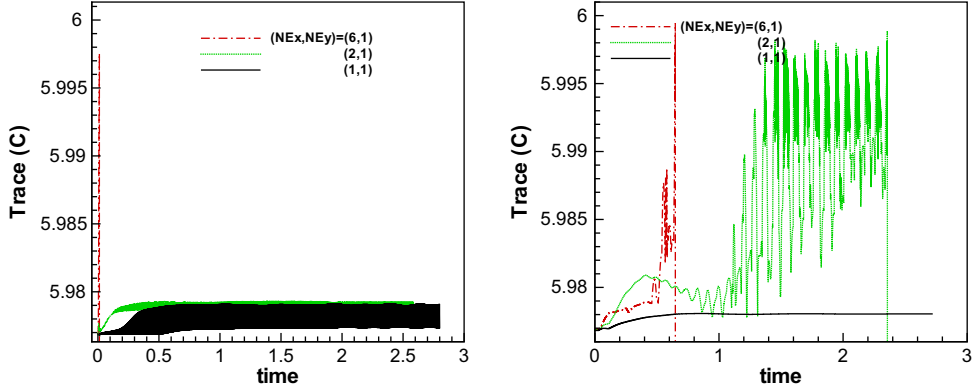


Fig. 18. Influence of mesh refinement on the maximum of $tr(C)$, $(N_x, N_y) = (4, 10)$, $We = 100$, natural outflow boundary condition: (left) $\Delta t = 0.002$, (right) $\Delta t = 0.0002$.

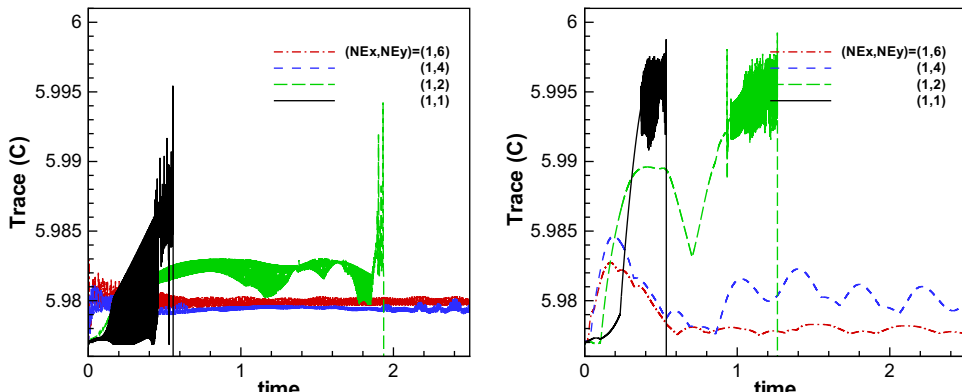


Fig. 19. Influence of mesh refinement on the maximum of $tr(C)$, $(N_x, N_y) = (10, 5)$, $We = 100$, natural outflow boundary condition: (left) $\Delta t = 0.002$, (right) $\Delta t = 0.0002$.

maximum value is close to $b^2 = 6$, which makes the simulation extremely difficult for this value of the Weissenberg number. Indeed, by the smallest oscillation of the trace of the conformation, the value of viscoelastic stress grows unbounded which is the worst condition in the simulation of viscoelastic fluids. Since the difference

between the results corresponding to this time interval and the smaller one, $\Delta t = 0.0002$ is indistinguishable, only the ones related to $\Delta t = 0.002$ are shown.

The next two test cases indicate the effect of mesh refinement by increasing the polynomial degree at $\Delta t = 0.002$ and

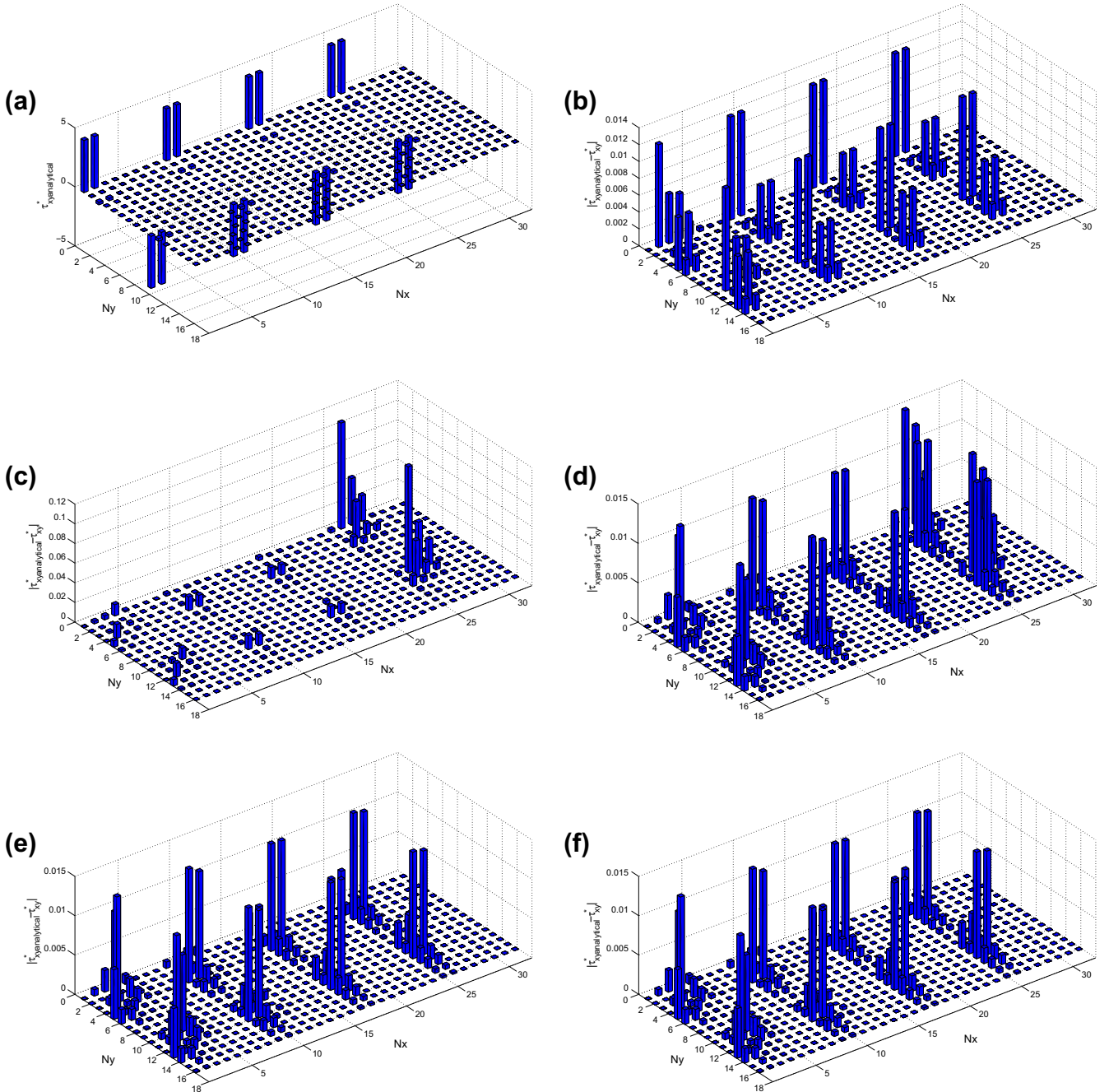


Fig. 20. Typical variation of modal spectrum of τ_{xy} with time evolution after applying filtering at $b^2 = 6$, $We = 1$, $(NE_x, NE_y) = (4, 2)$, $(N_x, N_y) = (7, 7)$ and natural outflow boundary condition: (a) full analytical prescription of the steady flow, (b) time step = 1, (c) time step = 181, (d) time step = 301, (e) time step = 1001, (f) time step = 3000.

Table 6

Maximum variation of modal spectrum of τ_{xy} with time evolution after applying filtering at $b^2 = 6$, $We = 1$, $(NE_x, NE_y) = (4, 2)$ and natural outflow boundary condition.

	Time step	1	11	131	301	401	1001	1501	2541	3001
$(N_x, N_y) = (10, 10)$	$ \tau_{xy\text{analytical}}^* - \tau_{xy}^* $	0.01	0.14	0.50	–	–	0.01	–	–	0.01
$(N_x, N_y) = (15, 15)$	$ \tau_{xy\text{analytical}}^* - \tau_{xy}^* $	0.01	–	–	0.01	1.40	–	14.00	35.00	–

$\Delta t = 0.0002$. Fig. 16 shows the effect of mesh refinement in stream-wise direction at $We = 100$ and (4×2) elements in the stream-wise and cross-wise directions. As it is clear in this figure, increasing the polynomial degree in the stream-wise direction, enhances the value of the trace of the conformation tensor sharply. For polynomial degrees (10×5) and (8×5) the maximal values of the trace of the conformation tensor are still less than the selected bounded value of the conformation tensor, $b^2 = 6$, but they are close enough to the bounded value according to the precision of the computer. In this region, unphysical values of viscoelastic stress are achieved which enforces the computation to blow up. The significant difference between these two time intervals is that at $\Delta t = 0.002$, the appearance of instability occurs at low time t , while for the smaller time interval the start point of instability is postponed till $t = 2$.

Fig. 17 shows the effect of mesh refinement by increasing the polynomial degree in the cross-wise direction at $We = 100$ and (4×2) element in the stream-wise x and cross-wise y directions, respectively. Increasing the polynomial degree in the y direction produces large oscillations during the computation at $\Delta t = 0.002$ while at $\Delta t = 0.0002$ increasing the polynomial degree does not have any significant effect.

The last two test cases are devoted to the examination of mesh refinement effects by increasing the number of elements in both x and y directions at $We = 100$. Fig. 18 represents the influence of refining the mesh on the trace of the conformation tensor by increasing the number of element in stream-wise direction with (4×10) polynomial degrees respectively in the stream-wise and cross-wise directions. In the y direction, we chose a large value

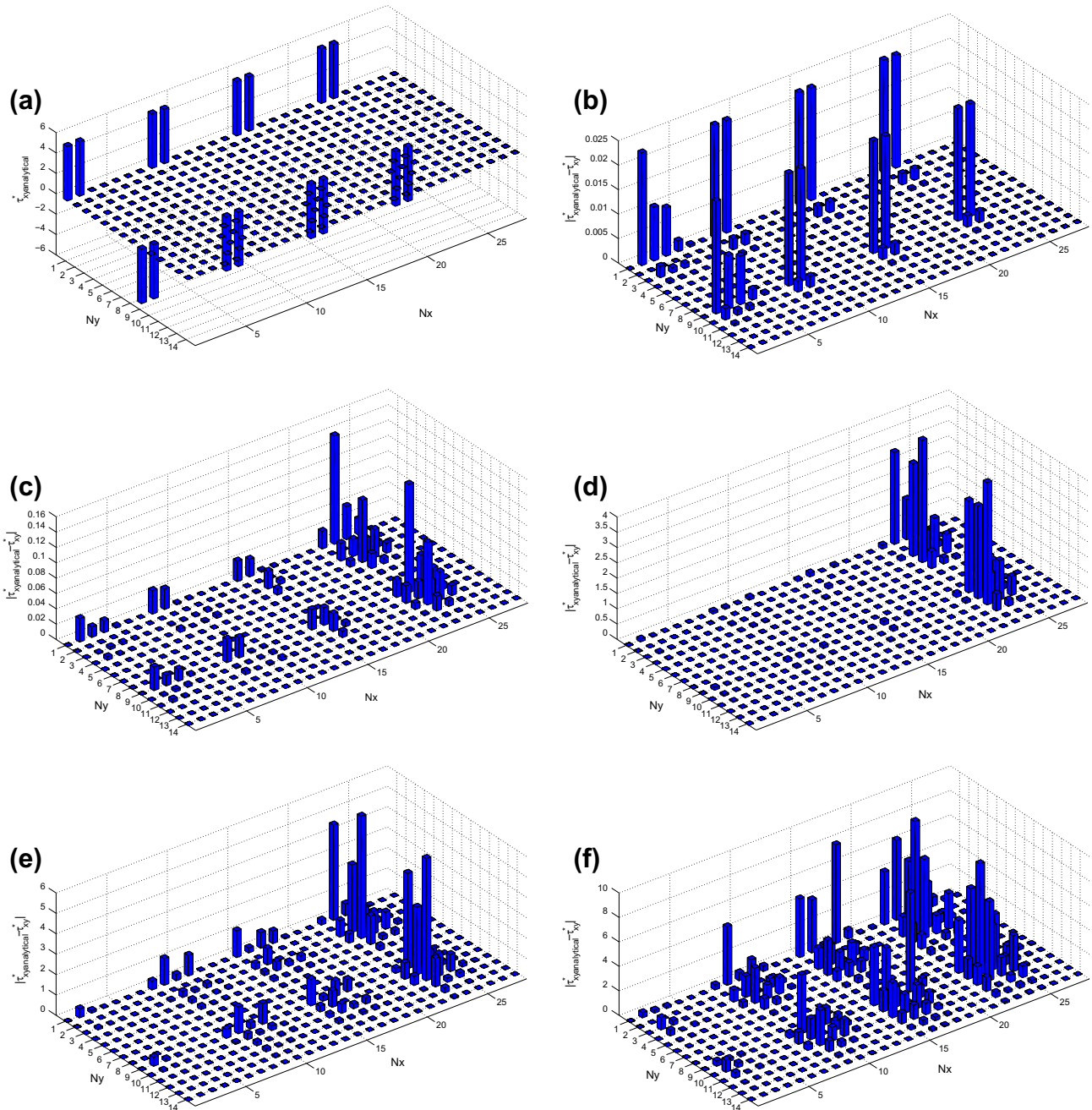


Fig. 21. Typical variation of modal spectrum of τ_{xy} with time evolution after applying filtering at $b^2 = 6 \times 10^6$, $We = 1$, $(NE_x, NE_y) = (4, 2)$, $(N_x, N_y) = (6, 6)$ and natural outflow boundary condition: (a) full analytical prescription of the steady flow, (b) time step = 1, (c) time step = 101, (d) time step = 1001, (e) time step = 2001, (f) time step = 3000.

of the polynomial degree to ensure an acceptable refined mesh in this direction. In this test case, as before, increasing the number of element increases the maximum value of the trace of the conformation tensor as well as the magnitude of the oscillations during the simulation. For small values of the time step, the instability appears later.

Fig. 19 shows the effect of mesh refinement by increasing the number of elements in the cross-wise direction by (10×5) polynomial degree in the stream-wise and cross-wise directions. A polynomial degree equal to 10 in the x direction is selected in order to obtain an enough refined mesh. The great difference between this figure and the previous ones is that increasing the number of element in cross-wise direction, stabilizes the simulation and decreases the oscillation of maximum trace of conformation tensor

during time evolution. Moreover, smaller time interval improves the behavior of the results with time evolution.

8. Results with filtering

8.1. Influence of the filter-based stabilization of the spectral element method

After reporting about the mechanisms of instability and investigating the effect of different physical and discretization parameters on the growth of instabilities, let us inspect the effect of filter-based stabilization techniques. Such stabilization can be carried out either in modal basis [1] or in nodal basis [27]. In this study,

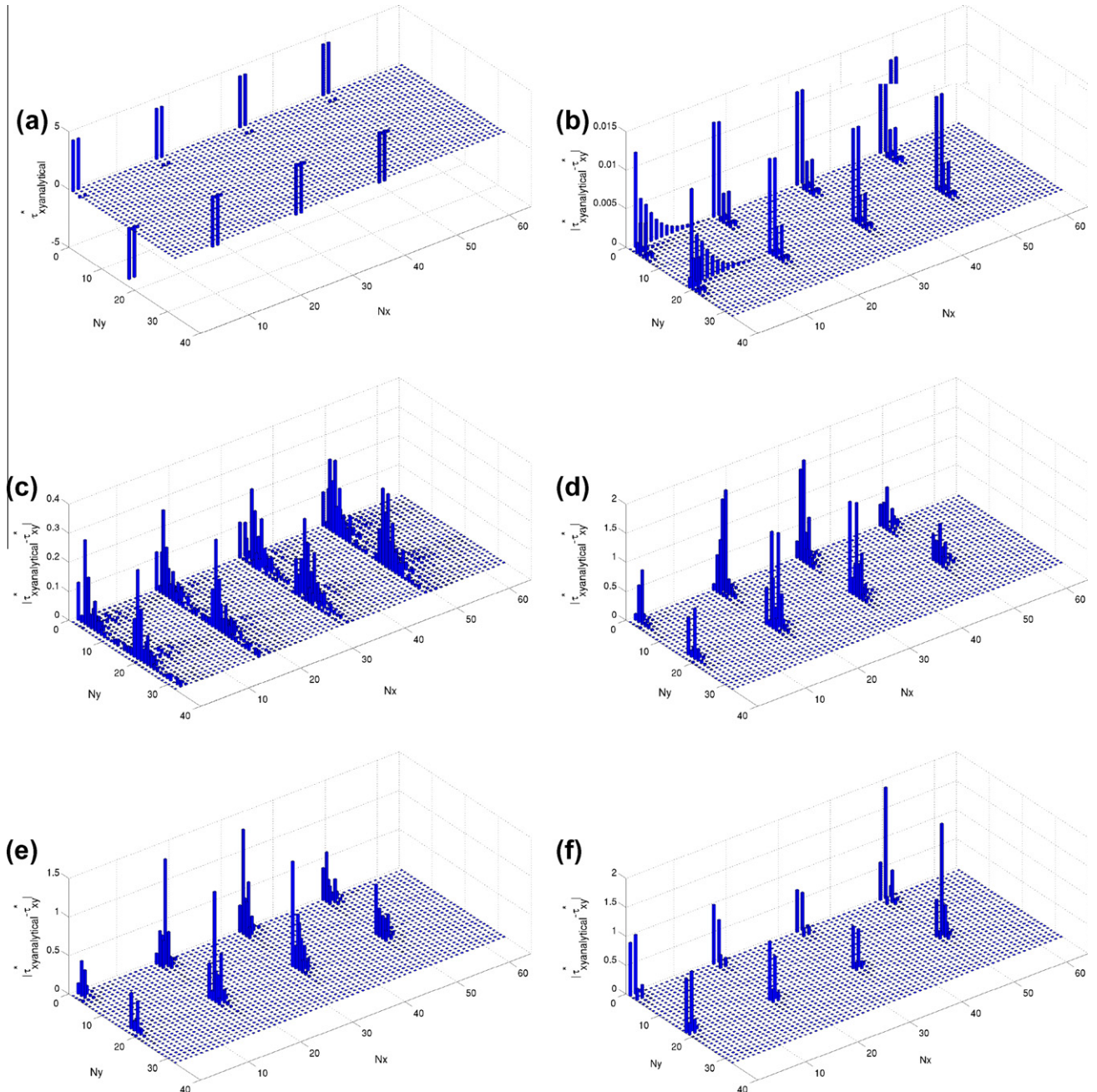


Fig. 22. Typical variation of modal spectrum of τ_{xy} with time evolution and mesh-transfer technique, FENE-P, $We = 1$, $(NE_x, NE_y) = (4, 2)$, $(N_x, N_y) = (15, 15)$ and natural outflow boundary condition: (a) full analytical prescription of the steady flow, (b) time step = 1, (c) time step = 1001, (d) time step = 2001, (e) time step = 3001, (f) time step = 4000.

we only considered the former stabilization technique proposed by Boyd. The results reported in this section are obtained for multi-element configurations and those obtained by single element have been skipped for the sake of conciseness. To enable one to compare the results, for different cases, only the modal spectrum of the viscoelastic shear stress component is shown. The same behavior with respect to the growth of instabilities can be observed with the stream-wise velocity and viscoelastic normal stress components in the 2-D Poiseuille flow. The details about the parameters used in the filtering technique and shape functions have been presented in Section 4.1.

Regarding the previous analysis, concerning the effect of mesh refinement at $We = 1$ for (4×2) elements in the stream and cross-wise directions, the maximum polynomial degrees in both

direction enabling completion of the simulation up to 5000 time steps with time step $\Delta t = 0.002$ and natural outflow boundary condition successfully is (6×6) , if no filtering is used. To check the capability of this filter based technique we start with polynomial degree (7×7) . Fig. 20 represents the effect of applying the considered filter at each time step during the simulation. Even though this filter is useful to eliminate spurious modes, there are still some unphysical modes that remain till the end of the simulation leading to an error of the order of $O(10^{-2})$ and decrease the accuracy of results. Comparing this result with Fig. 7 clarifies the difference between filtered and non-filtered cases for the same conditions. As it is obvious in Fig. 7, simulation without employing filtering for (7×7) polynomial degree stops after 103 time steps because of the presence of the unstable modes of magnitude of order $O(10^3)$.

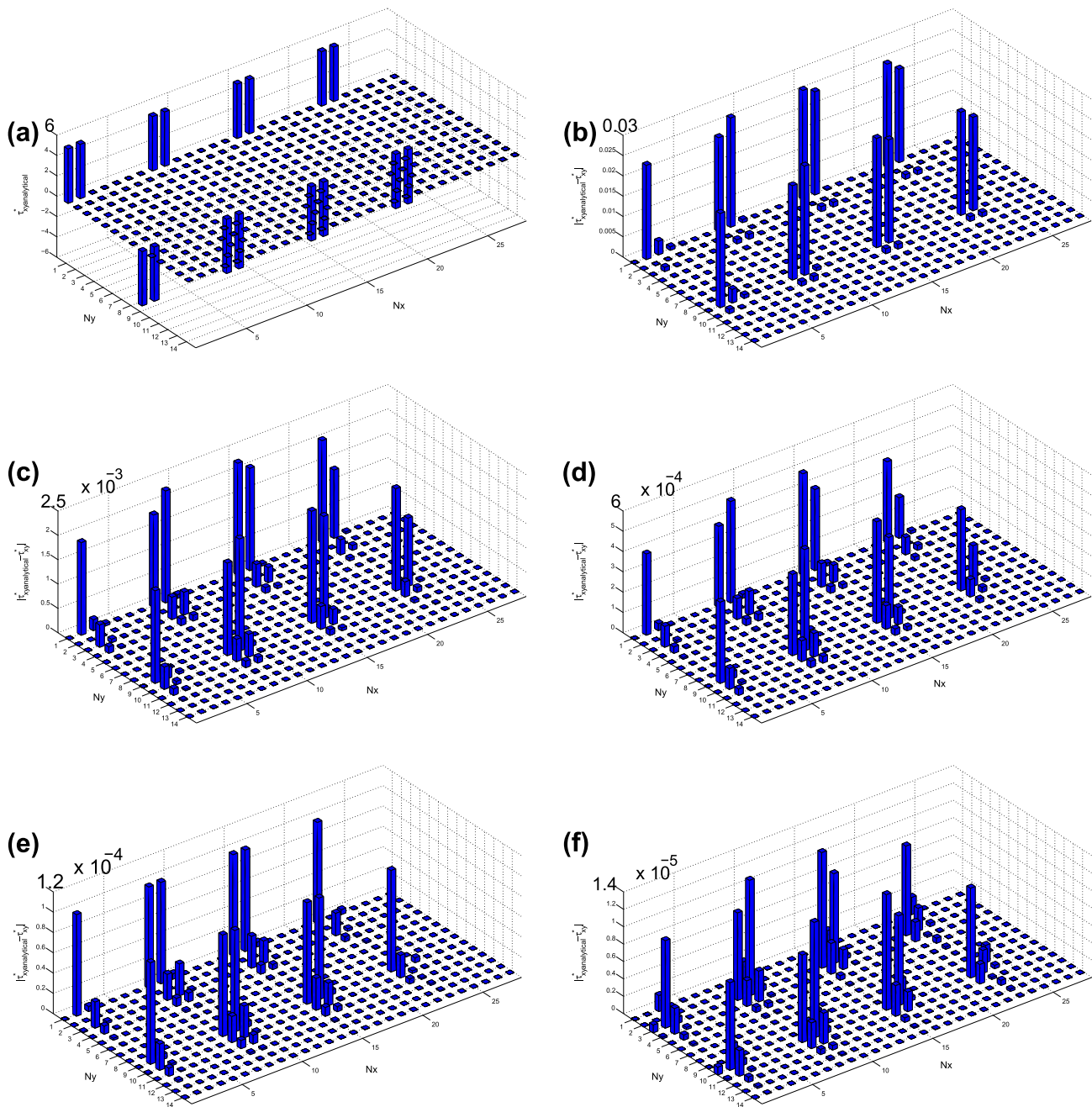


Fig. 23. Typical variation of modal spectrum of τ_{xy} with time evolution and mesh-transfer technique, Oldroyd-B, $We = 1$, $(NE_x, NE_y) = (4, 2)$, $(N_x, N_y) = (6, 6)$ and natural outflow boundary condition: (a) full analytical prescription of the steady flow, (b) time step = 1, (c) time step = 1001, (d) time step = 2001, (e) time step = 3001, (f) time step = 4000.

Table 6 also indicates the effect of imposing of filter based stabilization technique for (10×10) and (15×15) polynomial degrees and (4×2) elements in the stream-wise and cross-wise directions. Applying this filter for polynomial order (10×10) also cures the significant unphysical modes, but for polynomial degree (15×15) employing filter based technique only postpones the fast growth of disturbing modes and after 2541 iterations, the simulation stopped.

The effect of filter based stabilization technique for Oldroyd-B fluids is shown in Fig. 21. Oldroyd-B is considered as a particular case of the FENE-P model when $b \rightarrow \infty$. This test case corresponds to (4×2) elements and (6×6) polynomial degree in stream and cross-wise direction at $We = 1$ and a natural boundary condition. After 3000 iterations with $\Delta t = 0.002$, because of the appearance of spurious modes of magnitude order $O(10)$, the simulation ended. However, without employing the filter-based technique simulation stopped only after 121 iterations (Fig. 10), but applying filtering only postpones the development of disturbing modes.

8.2. Influence of mesh-transfer technique

What we observed in the previous section was that applying the filter-based stabilization technique as such on the elements for the FENE-P model could be useful to damp and eliminate spurious modes, but at the end of the simulation, the effect of some spurious modes still remains. Applying this filter for the Oldroyd-B model corresponding to an infinite value of the extensibility parameter only postpones the time of blowing up of the numerical simulation and the performance of this technique is not ideal for the Oldroyd-B case. According to our observation, we found that the performance of this technique while using a one element decomposition is better than for a multi-element decomposition. Probably, multi-element decomposition is an obstacle for this technique due to the presence of interfaces between elements. One possible remedy to solve the associated problem of multi-element decomposition is to employ a mesh-transfer technique. As we explained in Section 5, at each time step, one has to map a multi-element configuration to a single element configuration, on which one applies the filter-based stabilization technique and then transfers back the filtered fields to the first (multi-element) topology. To show relevant results, we have selected three different test cases. Fig. 22 represents the results for FENE-P model for (15×15) polynomial degree, while Fig. 23 and Table 7 correspond to the same test cases for Oldroyd-B with (6×6) and (15×15) polynomial degrees respectively. These test cases have been carried out for (4×2) elements in the stream-wise and cross-wise directions and with a natural outflow boundary condition for $We = 1$ and $\Delta t = 0.002$.

In Fig. 22, at each time step first we map a topology with (4×2) elements and (15×15) polynomial degrees to a single element with (61×61) polynomial orders, then we apply filter-based stabilization for this simple topology and afterwards transfer back each filtered variable to the original configuration. To preserve the spectral accuracy we map the multi-element configuration to a single one with polynomial orders at least corresponding to the maximum number of nodes for multi-element configuration in each direction. In the above configuration, the number of nodes in stream and cross-wise direction are 61 and 31 respectively. Thus, the selected single element topology with (61×61) polyno-

mial degrees satisfies this accuracy criterion. Comparison between Fig. 22 and Table 6 reveals that applying mesh-transfer technique enhances the performance of filter-based stabilization and also decreases the penetration of disturbing waves. After 4000 time steps the order of the error if the mesh-transfer technique is used, is $O(1)$ as shown in Fig. 22, while without employing the mesh-transfer technique, the order of the error after 2541 iterations in Table 6 is $O(10)$.

In Fig. 23, first we map (4×2) and (6×6) element and polynomial degree configuration to a new topology with one element and (25×25) polynomial degrees, apply the filtering and transfer back to the original mesh. Results clearly reveal that employing mesh-transfer technique for Oldroyd-B is very efficient. The order of error of modal spectrum of shear viscoelastic stress after 4000 iterations is $O(10^{-5})$, a value impossible to be obtained while using the stabilization technique without mesh transfer as it can be observed in Fig. 21.

The same behavior is also observed in Table 7. Again we transfer our configuration, (4×2) elements with (15×15) , to a single element by (61×61) polynomial degree. This time dependent simulation has been done for 4000 time steps with $\Delta t = 0.002$. The maximum relative error at the end of the simulation is ordered of $O(10^{-3})$, which is less accurate than the previous test case. We can conclude that this way of implementing filtering is very useful for the Oldroyd-B model when a moderate number of points is used in the one element intermediate grid.

9. Conclusion

In order to investigate the numerical instability generation in the simulation of flows of FENE-P family, a comprehensive study about the growth of spurious modes with time evolution, Weissenberg number, mesh refinement, finite extensibility parameter and outflow boundary condition has been done using a modal basis representation. Increasing the Weissenberg number usually leads to the manifestation of numerical instabilities in the simulation of viscoelastic fluid flows. For a multi-element decomposition, the instability first appears in elements close to the outflow region and propagates very fast upstream. Mesh refinement enhances the growth of spurious modes in the domain. This is the reason why refining the mesh proved to be not helpful for computing viscoelastic flows. Increasing the finite extensibility parameter enhances the magnitude of dangerous modes and causes simulation crashes. The effect of the outflow boundary condition reveals that the instability is highly sensitive to the corresponding choice. Applying a velocity Dirichlet condition at outflow as opposed to a natural one was found better in terms of convergence and stabilization. Imposing condition of the latter type at outflow governs the system not only by the state in the interior of the region, but also by the information brought by incoming characteristics which enter the region. Probably this is the reason why applying a natural condition induces the generation of instabilities first in the outflow region.

The capability of filter-based-stabilization technique proposed by Boyd [1] has been examined. Although this filter is capable to suppress the high frequency modes, there are still some nascent instabilities which grow by mesh refinement, therefore applying a filter-based technique cannot treat the instability problem completely. We also observed that the performance of filter-based stabilization technique is very useful to eliminate spurious modes for one element decomposition, while in the case of multi-element configuration the performance of this technique is not ideal. Regarding this fact, a new way of implementation based on the mesh-transfer technique is used. This algorithm is very useful for Oldroyd-B when a moderate number of grid points is used.

Table 7

Maximum variation of modal spectrum of τ_{xy} with time evolution and mesh-transfer technique, Oldroyd-B, $We = 1$, $(NE_x, NE_y) = (4, 2)$, $(N_x, N_y) = (15, 15)$ and natural outflow boundary condition.

Time step	1	1001	2001	3001	4000
$ \tau_{xy}^* - \tau_{xy} $	0.03	0.01	4×10^{-3}	1.10×10^{-3}	10^{-3}

We also showed that however preserving the symmetric positive definiteness of the conformation tensor and bounding the trace of the conformation tensor to a value lower than the finite extensibility parameter, helps to obtain stable computations but another problem that can easily appear is that the attained value of trace of conformation tensor tends to the corresponding bounded value related to the finite extensibility. Due to the presence of the term $1 - \text{tr}(C)/b^2$ in the denominator of the viscoelastic stress formulation of FENE-P, tends to zero, this causes unbounded growth of the viscoelastic stress, which does not have any physical meaning. Indeed, by the smallest oscillation of the trace of the conformation, the value of viscoelastic stress grows unbounded which is the worst condition of the simulation of viscoelastic fluids. Mesh refinement in the stream-wise direction by increasing both polynomial degrees or number of elements, increases the maximum value of the trace of the conformation tensor which makes the simulation to reach the dangerous zone and finally uncontrolled instabilities are generated. Mesh refinement in the cross-wise direction by increasing the polynomial degree has the same effect, while mesh refinement in the cross-wise direction by increasing the number of elements has the opposite effect. The main difference is that increasing the number of elements in the cross-wise direction, stabilizes the simulation and decreases the oscillation amplitude of the trace of the conformation tensor with time. Moreover, selecting a smaller time interval improves the behavior of the results with time evolution. Regarding the transformation suggested by Fattal and Kupferman [35] and Van Os and Phillips [50], symmetric positive definiteness (SPD) is preserved during the simulation but overflow and underflow numerical errors happen when the classical conformation is reconstructed from exponential formulation with either infinite positive eigenvalue or infinite negative eigenvalue using the logarithm formulation. Thus, the development of mathematical models to preserve both SPD of the conformation tensor and bound the magnitude of eigenvalues when reconstructing the classical formulation is mandatory. Such an investigation is underway.

Employing this mesh transfer filtering technique for complex geometry such as 2-D contraction flow will be considered in a future work. Furthermore, according to the fact that one of the main reasons for instability generation in the simulation of the time dependent Poiseuille flow is the reflection of outgoing waves from the outflow boundary, it would be beneficial to resort to a 2-D spatial discretization that would use spectral elements in the cross-wise direction coupled with a Fourier expansion in the stream-wise direction imposing that the flow would be periodic. This is left for a future study.

Acknowledgments

We are grateful to Dr. Roland Bouffanais for his precious advice and guidance for the mesh update technique. This research was funded by a Swiss National Science Foundation Grant (No. 200020-112085) whose support is gratefully acknowledged.

References

- [1] Boyd JP. Two comments on filtering (artificial viscosity) for Chebyshev and Legendre spectral and spectral element methods: preserving boundary conditions and interpretation of the filter as a diffusion. *J Comput Phys* 1998;143(1):283–8.
- [2] Joseph DD, Renardy M, Saut JC. Hyperbolicity and change of type in the flow of viscoelastic fluids. *Arch Ration Mech Anal* 1985;87:213–51.
- [3] Joseph D, Saut J. Change of type and loss of evolution in the flow of viscoelastic fluids. *J Non-Newt Fluid Mech* 1986;20:117–41.
- [4] Owens RG, Phillips TN. Computational rheology. London: Imperial College Press; 2002.
- [5] Deville MO, Fischer PF, Mund EH. High-order methods for incompressible fluid flow. Cambridge: Cambridge University Press; 2002.
- [6] Marchal JM, Crochet M. A new mixed finite element for calculating viscoelastic flow. *J Non-Newt Fluid Mech* 1987;26:77–114.
- [7] Rosenberg J, Keunings R. Numerical integration of differential viscoelastic models. *J Non-Newt Fluid Mech* 1991;39:269–90.
- [8] Brooks AN, Hughes TJR. Streamline upwind Petrov–Galerkin formulations for convection dominated flows with particular emphasis on the incompressible Navier–Stokes equations. *Comput Methods Appl Mech Eng* 1982;32:199–259.
- [9] Chauvière C, Owens RG. A new spectral element method for the reliable computation of viscoelastic flow. *Comput Methods Appl Mech Eng* 2001;190:3999–4018.
- [10] Chauvière C, Owens RG. Wiggle-free spectral element methods for non-Newtonian flows. In: Deville M, Owens RG, editors. Proceedings of the 16th IMACS world congress, Lausanne, Switzerland; 2000.
- [11] Fortin M, Fortin A. A new approach for the fem simulation of viscoelastic flows. *J Non-Newt Fluid Mech* 1989;32:295–310.
- [12] Johnson C, Nåvert U, Pitkäraanta J. Finite element methods for linear hyperbolic problems. *Comput Methods Appl Mech Eng* 1984;45:285–312.
- [13] Gerritsma MI, Phillips TN. Discontinuous spectral element approximations for the velocity–pressure–stress formulation of the Stokes problem. *Int J Numer Methods Eng* 1998;43:1401–19.
- [14] Gerritsma MI, Phillips TN. Compatible spectral approximations for the velocity–pressure–stress formulation of the Stokes problem. *SIAM J Sci Comput* 1999;20(4):1530–50.
- [15] Schaftingen JV, Crochet MJ. A comparison of mixed methods for solving the flow of a Maxwell fluid. *Int J Numer Methods Fluids* 1984;4:1065–81.
- [16] Chang BFPW, Patten TW. Collocation and Galerkin finite element methods for viscoelastic fluid flow – i: description of method and problems with fixed geometry. *Comput Fluids* 1979;7:267–83.
- [17] Rajagopalan D, Armstrong R, Brown R. Finite element methods for calculation of steady, viscoelastic flow using constitutive equations with a Newtonian viscosity. *J Non-Newt Fluid Mech* 1990;36:159–92.
- [18] Khomami B, Talwar KK, Ganpule HK. A comparative study of higher- and lower-order finite element techniques for computation of viscoelastic flows. *J Rheol* 1994;38(2):255–89.
- [19] Guénette R, Fortin M. A new mixed finite element method for computing viscoelastic flows. *J Non-Newt Fluid Mech* 1995;60(1):27–52.
- [20] Fan Y, Tanner RL, Phan-Thien N. Galerkin/least-square finite-element methods for steady viscoelastic flows. *J Non-Newt Fluid Mech* 1999;84(2–3):233–56.
- [21] Franca LP, Stenberg R. Error analysis of some Galerkin least squares methods for the elasticity equations. *SIAM J Numer Anal* 1991;28(6):1680–97.
- [22] Gerritsma M. Direct minimization of the discontinuous least-squares spectral element method for viscoelastic fluids. *J Sci Comput* 2006;27(1–3):245–56.
- [23] Surana K, Bhola S, Reddy J, TenPas P. k-version of finite element method in 2d-polymer flows: upper convected Maxwell model. *Comput Struct* 2008;86(17–18):1782–808.
- [24] Canuto C, Russo A, van Kemenade V. Stabilized spectral methods for the Navier–Stokes equations: residual-free bubbles and preconditioning. *Comput Methods Appl Mech Eng* 1998;166:65–83.
- [25] Funaro D. A new scheme for the approximation of advection-diffusion equations by collocation. *SIAM J Numer Anal* 1993;30(6):1664–76.
- [26] Ma X, Symeonidis V, Karniadakis G. A spectral vanishing viscosity method for stabilizing viscoelastic flows. *J Non-Newt Fluid Mech* 2003;115(2–3):125–55.
- [27] Fischer P, Mullen J. Filter-based stabilization of spectral element methods. *CR Acad Sci Paris* 2001;332:265–70.
- [28] Fischer PF, Kruse GW, Loth F. Spectral element methods for transitional flows in complex geometries. *J Sci Comput* 2002;17(1):81–98.
- [29] Dubois-Pelerin Y, Van Kemenade V, Deville MO. An object-oriented toolbox for spectral element analysis. *J Sci Comput* 1999;14:1–29. <<http://sourceforge.net/projects/openspeculoos/develop>>.
- [30] Bird RB, Armstrong RC, Hassager O. Dynamics of polymeric liquids, vol. 1. New York: Wiley; 1987.
- [31] Keunings R. On the Peterlin approximation for finitely extensible dumbbells. *J Non-Newt Fluid Mech* 1997;68(1):85–100.
- [32] Bird RB, Dotson PJ, Johnson NL. Polymer solution rheology based on a finitely extensible bead-spring chain model. *J Non-Newt Fluid Mech* 1980;7:213–35.
- [33] Vaithianathan T, Collins LR. Numerical approach to simulating turbulent flow of a viscoelastic polymer solution. *J Comput Phys* 2003;187:1–21.
- [34] Jafari A, Fiétier N, Deville MO. A new extended matrix logarithm formulation for the simulation of viscoelastic fluids by spectral elements. *Comput Fluids* 2010;39:1425–38.
- [35] Fattal R, Kupferman R. Time-dependent simulation of viscoelastic flow at high Weissenberg number using the log-conformation representation. *J Non-Newt Fluid Mech* 2005;126:23–37.
- [36] Fattal R, Kupferman R. Constitutive laws for the matrix-logarithm of the conformation tensor. *J Non-Newt Fluid Mech* 2004;123:281–5.
- [37] Jafari A. Simulation of time-dependent viscoelastic fluid flows by spectral elements. Ph.D. thesis, Ecole Polytechnique Fédérale de Lausanne; 2011 [no. 4955].
- [38] Fiétier N, Deville MO. Time dependent algorithms for simulation of viscoelastic flows with spectral element methods: applications and stability. *J Comput Phys* 2003;186:93–121.
- [39] Perot JB. An analysis of the fractional step method. *J Comput Phys* 1993;108:51–8.
- [40] Gjesdal T, Wasberg C, Reif B. Spectral element benchmark simulations of natural convection in two-dimensional cavities. *Int J Numer Methods Fluids* 2006;50(11):1297–319.

- [41] Xu C, Maday Y. A spectral element method for the time-dependent two-dimensional Euler equations: applications to flow simulations. *J Comput Appl Math* 1998;91(1):63–85.
- [42] Black K. Approximation of Navier–Stokes incompressible flow using a spectral element method with a local discretization in spectral space. *Numer Methods Part Differ Eqns* 1997;13(6):587–99.
- [43] Ho L-W, Rønquist E. Spectral element solution of steady incompressible viscous free-surface flows. *Finite Elem Anal Des* 1994;16(3–4):207–27.
- [44] Xu C. Stabilization methods for spectral element computations of incompressible flows. *J Sci Comput* 2006;27:495–505.
- [45] Bouffanais R. Simulation of shear-driven flows: transition with a free surface and confined turbulence. Ph.D. thesis, Ecole Polytechnique Fédérale de Lausanne; 2007 [no. 3837].
- [46] Stoltz S, Adams N, Kleiser L. The approximate deconvolution model for large-eddy simulations of compressible flows and its application to shock-turbulent-boundary-layer interaction. *Phys Fluids* 2001;13:2985–3001.
- [47] Stoltz S, Adams N, Kleiser L. An approximate deconvolution model for large-eddy simulation with application to incompressible wall-bounded flows. *Phys Fluids* 2001;13(4):997–1015.
- [48] Waters ND, King MJ. The unsteady flow of an elasto-viscous liquid in a straight pipe of circular cross section. *J Non-Newt Fluid Mech* 1971;4: 204–11.
- [49] Bouffanais R, Deville MO. Mesh update techniques for free-surface flow solvers using spectral element method. *J Sci Comput* 2006;27(1–3):137–49.
- [50] Van Os RGM, Phillips TN. Spectral element methods for transient viscoelastic flow problem. *J Comput Phys* 2004;201:286–314.